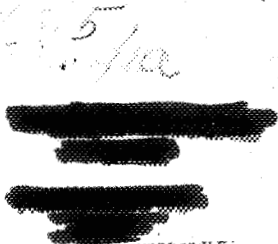


MAY 29 1945

superseded by
revised report



NATIONAL ADVISORY COMMITTEE FOR AERONAUTICS

rec'd 8-31-45

CASE FILE COPY

CLASSIFICATION CANCELLED

Authority W. L. Alderden Date 6/21/56
Dir. Aeron. Research
NACA

By CAF M. F. Schmitt 551
Status Inactive

MEMORANDUM REPORT

for the

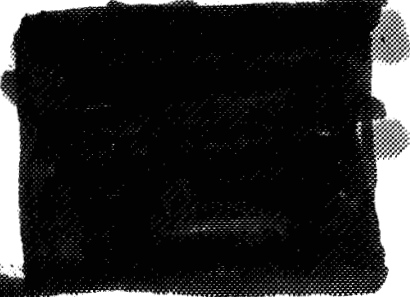
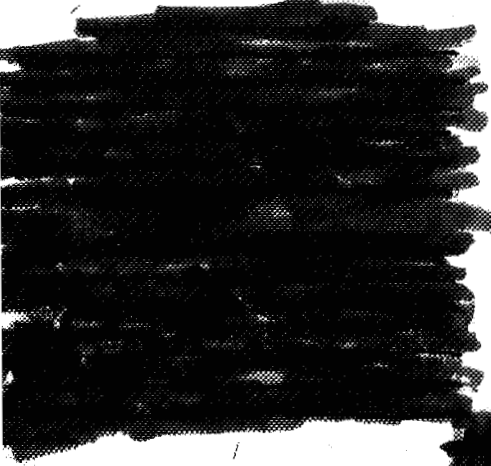
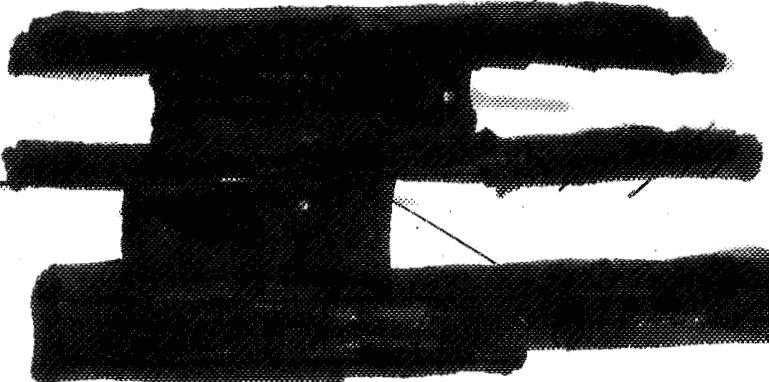
Bureau of Aeronautics, Navy Department

NACA

AN EXPERIMENTAL INVESTIGATION OF SUBMERGED-
DUCT ENTRANCES

By Charles W. Frick, Wallace F. Davis, Lauros Randall,
and Emmet A. Mossman

Ames Aeronautical Laboratory
Moffett Field, Calif.



May 23, 1945

~~CLASSIFICATION~~ CANCELLED

NATIONAL ADVISORY COMMITTEE FOR AERONAUTICS

MEMORANDUM REPORT

for the

Bureau of Aeronautics, Navy Department

AN EXPERIMENTAL INVESTIGATION OF ^{NACA} SUBMERGED-
DUCT ENTRANCES

By Charles W. Frick, Wallace F. Davis, Lauros Randall,
and Emmet A. Mossman

SUMMARY

The results of an investigation of submerged-duct entrances are presented. It is shown that this type of entrance possesses the following characteristics:

1. Very high-critical-compressibility speeds throughout the range of high-speed inlet-velocity ratios
2. Very low pressure losses for the air entering the duct at all inlet-velocity ratios
3. Low external drag

These characteristics are obtained by the proper shaping of the contour of the upstream approach to the submerged inlets and by proper alignment of the duct lip. Design data are presented and the application of these data to a specific high-speed fighter-airplane design is discussed.

INTRODUCTION

The use of the jet-propulsion motor has greatly

~~CLASSIFICATION~~ CANCELLED

intensified the need for efficient air-induction systems for high-speed aircraft. Although the air quantities used by such motors are not greatly in excess of the over-all air requirements of conventional aircraft engines of equivalent high-speed thrust, the performance of a jet motor is affected to a much greater extent by pressure losses in the air-induction system resulting from poor design. At high speed, a loss in total pressure of 10 percent of the free-stream dynamic pressure for the air supplied to the jet motor of a typical fighter aircraft may result in a loss in thrust equivalent to about one-tenth of the airplane drag. When it is realized that very few of the air-induction systems of existing jet-propelled aircraft have total pressure recoveries of more than 65 percent of the free-stream dynamic pressure, it becomes apparent that there is a great need for improved designs.

The problem of obtaining low pressure losses for the air supplied to the jet motor is made more difficult by the necessity of obtaining these low losses without impairing the critical-compressibility speed or excessively increasing the drag of the basic airplane by protuberances or changes in the basic contour. It is quite possible through the use of large external scoops to obtain very satisfactory internal-air-flow characteristics, but the gain in jet-motor performance may be offset by the high drag resulting from the formation of local shock waves or by the excessive drag of the air scoops themselves.

Consideration of the problem has indicated that the use of air inlets submerged below the basic contour of the aircraft would eliminate the large drag of external air scoops. These submerged openings would also render the attainment of high-critical speed for the air inlets easier. It was anticipated that it would be difficult to obtain low internal-flow losses for the submerged scoop because of the necessity of diverting the air from its path along the surface into the submerged entrance. It was expected, also, that the existence of a boundary layer of low energy air along the surface into which the entrance was placed would make it difficult to attain low pressure losses. The cursory investigation of reference 1 confirmed this conclusion. It was believed, however, that through a proper selection of the contours of the surface upstream from the opening, the flow characteristics of the submerged opening could be improved to an extent which would permit an over-all increase in airplane performance. An experimental investigation was therefore undertaken.

[Essen, Theory of duct forms] - design
MODEL AND APPARATUS

The general investigations of the submerged entrances were made in the 1- by 1.5-foot wind channel shown in figure 1. This wind channel is of the open-return type and is powered with a high-capacity centrifugal blower capable of producing a maximum airspeed of 180 miles per hour in the test section.

The air stream itself is very smooth and probably of low turbulence because of the contraction ratio of 13.0 to 1.0.

Measurements of the tunnel air stream indicated an appreciably thick boundary on the walls of the test section. In order to obtain the thinnest boundary layer possible, a false wall was built into the wind-tunnel test section so that the tunnel-wall boundary layer passed between the false and true walls of the tunnel. The model submerged duct was placed in this false wall as shown in figure 1. Air flow into the model duct entrance was controlled through the use of a small centrifugal blower.

The model of the submerged duct entrance was so designed that the contours of the lip, the angle of the entrance ramp (fig. 1), and the divergence of the ramp could be changed without removing the other duct parts. The openings tested were of 4-square-inch area, one of 4- by 1-inch and the other 2- by 2-inch dimension. For all tests the air drawn into the entrance was expanded to a very low velocity in an 8° conical diffuser of 13.0 to 1.0 area ratio. Sketches of two of the entries tested are shown in figure 2.

A specific application of the results of the general investigation was tested on a 0.25-scale model of a fighter-type aircraft in the 7- by 10-foot wind tunnel. Views of the submerged duct for this model are shown in figures 3(a) and (b).

TESTS AND TEST METHODS

Measurements of the pressure losses of the air flowing into the submerged duct for the tests in the 1- by 1.5-foot wind channel were made both at the entrance and at the end of the diffuser. The placing of the total-pressure tubes and the static-pressure tubes in the entrance is shown in figure 4. Pressure losses at the end of the diffuser were measured with total-pressure tubes. It should be noted that all measurements of the pressure recovery at the end of the diffuser were made while the pressure-measuring tubes were located in the duct inlet. The pressure losses resulting from the drag of these rakes are of considerable magnitude and the data obtained for the diffuser are of comparative value only. This in no way detracts from the value of these measurements since they are used for comparing the effects of various changes to the entrance. Data useful to the designer were obtained with the rakes at the duct entrance. Losses measured with these rakes represent the values obtained with 100-percent diffuser efficiency. Data for other diffuser efficiencies may be computed from these measurements.

Pressure-distribution tests were made over the lip and the ramp of the entrance to permit an estimation of the critical speed. Pressure data obtained with flush orifices were used with reference 2 to obtain values of the critical Mach numbers for various operating conditions.

The effects of removing the boundary layer of the

surface ahead of the submerged duct were determined by testing suction slots at various locations ahead of the duct entrance. A small centrifugal blower was used to provide suction. Air quantities were measured with a calibrated venturi. A sketch of the boundary-layer-control test duct is shown in figure 5.

Nearly all tests were made by holding the tunnel airspeed constant and varying the air quantity flowing in the duct to vary the inlet-velocity ratio. A few tests were made at very high inlet-velocity ratios by reducing the tunnel airspeed.

Tests of submerged-duct entrances for the 0.25-scale model of the fighter aircraft were made by drawing the air ~~flowing into the ducts~~ ^{out} through a channel in the spar of the tip-supported model. The inlet-velocity ratio was held constant while the model angle of attack was varied. Pressure losses were measured at the simulated entrance to the Halford jet motor with a rake of 17 total-pressure-measuring tubes in each duct.

RESULTS AND DISCUSSION

General Investigation

The investigation of the submerged-duct entrances in the small wind channel was divided into phases, each concerned with one particular design variable. These variables were as follows:

1. Ramp design
2. Lip design

3. Entrance shape and aspect ratio
4. Boundary-layer thickness
5. Boundary-layer control
6. Drag

designer variables

The discussion deals with each of these variables separately.

The symbols used throughout this report are defined in the appendix. *[sketch showing elements]*

Ramp design.- During the preliminary tests of the submerged entrances, the pressure recoveries obtained both at the end of the diffuser and at the duct entrance were disappointingly low. A maximum value of pressure recovery of about 57 percent was measured after complete diffusion at an inlet-velocity ratio of 0.5. The pressure recovery decreased to zero when the inlet-velocity ratio was increased to a value of 1.3. The entrance tested consisted of a 1- by 4-inch opening at the end of a 7° ramp bounded by straight non-divergent walls. Since, at inlet-velocity ratios of less than 1.0, more air enters the upstream end of the ramp than flows into the entrance with resultant spillage over the sides and, since the streamlines of the flow diverge as the opening is approached, it was suggested that some improvement might be obtained by diverging the walls of the ramp to fit the streamlines more closely. Tests of the first divergent walls showed a surprising increase in the pressure recovery of 8 to 10 percent at inlet-velocity ratios of less than 1.0. To investigate this further, tests of various straight divergent

walls and one curved divergent wall as shown in figure 6 and table I were made. The results of these tests are shown in figure 7. The best pressure recoveries were obtained with the curved divergence 4 which gave a maximum pressure recovery of 73 percent at an inlet-velocity ratio of 0.40. A small improvement was found at inlet-velocity ratios greater than unity.

Examination of the pressure-loss data (fig. 8) obtained in the duct entrance shows that the effect of the divergent walls is to reduce appreciably the losses suffered by the air entering the duct. It was noticed, however, that while the pressure losses were much improved over the entrance as a whole, higher losses than those obtained with no divergence were found close to the ends in the ^{with description} upper half of the opening. This is shown by the data of figure 9 taken for the pressure rake mounted one-half inch from the end of the opening. Flow studies indicated that these pressure losses were originating in a short stalled region along the walls of the ramp. Attempts made to improve this by rounding the edges of the walls resulted in even greater losses. It was found that by placing small ridges or deflectors of a maximum height of one-half inch along the top of the divergent walls, as shown in figure 10, an appreciable gain in pressure recovery could be realized. When these were extended forward along the top of the wall to near the entrance to the ramp further improvement was realized at inlet-velocity ratios of less than 0.6. These

data are shown in figure 11. The combination of a curved divergence and the deflectors increased the maximum pressure recovery from 57 percent (fig. 7) to 78 percent (fig. 11) at an inlet-velocity ratio of 0.4 and from 20 percent to 36 percent at an inlet-velocity ratio of unity.

The above results were obtained with a ramp angle of 7° . It was necessary, therefore, to determine the effect of changing the ramp angle on the pressure losses and to find out whether the use of divergence was as efficacious with greater ramp angles as for 7° . The results of figure 12 show that, *from all the side walls*, without diverging walls, an appreciable improvement in the pressure recovery is experienced with increasing ramp angle especially at the inlet-velocity ratios greater than unity. The results of tests of various ramp angles with divergent walls presented in figure 13 show the effectiveness of the divergence in increasing the ramp angle up to 10° . For 15° , a large loss in pressure recovery was experienced.

[It should be explained that the measure of divergence used in this investigation is the ratio of the width of the entrance of the ramp to the width of the submerged entrance.] *earlier*

From the results of the tests, this appears to be a more important parameter than the angle of the walls. From the foregoing, it may be concluded that ramp angles up to 10° may be used without incurring excessive losses. The effectiveness of diverging the walls is the same for all ramp angles up to 10° , even though the pressure gradient along the ramp

10° to 15° what?
5 to 10 improved what about 120

floor increases slightly with the ramp angle (fig. 14).

Lip design.-- In designing a satisfactory lip for the submerged duct two requirements must be satisfied. First, the lip must have a shape such as to give a high-critical speed at low inlet-velocity ratios as are used in high-speed flight; and second, the lip shape must be such that no stalling of the internal flow will occur at high inlet-velocity ratios or even at infinite inlet-velocity ratio corresponding to the static ground operation of the jet motor. With these criteria in mind, seven lip shapes were tested. Line drawings of these shapes are given in figure 15 and tables II(a) and II(b) give their ordinates. The results of tests of these lip shapes are given in table III. The first lip tested was poor in all respects, especially insofar as the stalling of the internal flow was concerned. Adding curvature to the inner surface (lip 2) improved these stalling tendencies, but the critical speed was still very poor. Adding curvature to the outer surface (lip 3) did not improve the critical speed and made the internal-flow losses much greater. Adding curvature to both the inside and outside surface (lip 4) increased the critical speed and eliminated stalling of the lip except at infinite inlet-velocity ratio. Changing the nose radius (lip 5) did not improve this condition, but an increase in camber and an increase in nose radius resulted in an entirely satisfactory lip (lip 6). A further attempt to improve this lip

by increasing the lip radius still further resulted in decreased critical speeds. It is concluded that, for the duct tested, lip 6 was entirely satisfactory.

It was anticipated that changing the ramp of the submerged entrances might have an appreciable effect on the angle of flow at the lip and thereby on the critical speed. Tests of lip 6 with a ramp angle of 7° and divergence 4 showed a decrease in the maximum critical speed from 0.92 to a value of M_{cr} of 0.83 at an inlet-velocity ratio of 0.94. It was surmised that the increased pressure recovery with the divergent wall was increasing the angle of flow at the lip. While the value of M_{cr} of 0.83 is quite high under normal conditions, the fact that these submerged inlets probably will be used on surfaces over which the velocity is greater than free-stream velocity makes the attainment of the highest possible critical speed for the lip necessary for a satisfactory airplane installation.

To counteract the increased angle of flow, the lip of the duct was given 3° of down incidence. The effect of this change in incidence may be determined from a comparison of the pressure-distribution data of figures 16 and 17 which show the lip pressure with zero incidence and with 3° down incidence. The effect of the change on the critical Mach number is shown in figure 18. The maximum critical speed with 3° of down incidence is increased to a value of M_{cr} of 0.92 at an inlet-velocity ratio of 0.85.

It was anticipated further that a change in ramp angle might have an appreciable effect on the critical Mach number of the lip by changing the angle of flow. Data obtained for lip 6 shown in figures 16, 19, and 20 indicate a sizeable effect of ramp-angle change on the pressure distribution over the lip. It is possible to compensate for the change in ramp angle by changing the incidence of the lip. This is believed more desirable than changing the camber of the lip itself since it is possible that the contours of the lip may be changed enough to cause stalling of the internal flow at infinite inlet-velocity ratio.

The original lips used for the submerged ducts, as shown by figure 15(a), protruded slightly above the surface. This effect is not detrimental but it is somewhat easier to fair the ends of the lip and to change its incidence if it is lowered until its upper surface becomes tangent to the surface into which the submerged duct is placed, as shown by figures 2 and 15(b). Tests of this arrangement showed the same characteristics as for the original lip location. Ordinates for the lip so placed are given in table I(b).

Entrance aspect ratio.-- A few tests were made to determine the effect of entrance aspect ratio on the pressure-recovery characteristics. Comparative results are shown in figure 21 for the 1- by 4-inch opening (for which most of the research was conducted) and a 2- by 2-inch opening. The effectiveness of diverging the walls for the 2- by 2-inch opening is of

comparable magnitude to that found for the 1- by 4-inch entry. The maximum pressure recovery which may be realized for the 2- by 2-inch opening is slightly less than for the rectangular opening. The data of figure 22 indicate that the loss in pressure recovery resulting from a thick boundary layer is somewhat less for the square opening.

Effect of boundary-layer thickness.- All of the tests discussed above were made with the normal boundary layer of the false wall of the wind channel noted as boundary layer 1 in figure 23. In order to ascertain the effect of boundary-layer thickness and to provide data applicable to submerged-duct installations far aft on the fuselage of an airplane, tests were also made with the two other boundary-layer thicknesses shown in figure 23. Results of these tests are shown in figure 24. As expected, these thicker boundary layers appreciably reduced the apparent pressure recovery at the end of the diffuser.

In order to ascertain the effect of the deflectors on the pressure recovery, tests were made with both normal and extended deflectors. (See fig. 10.) The results of these tests are shown in figure 25. It may be seen that for the thinnest boundary layer, the normal deflectors showed an appreciable improvement while the extended deflectors improved the pressure recovery only for a small range of low inlet-velocity ratios. With boundary layer 2, the use of extended deflectors very appreciably increased the pressure recovery.

With boundary layer 3 the improvement resulting from the use of deflectors was less, due to the fact that the boundary layer was very thick.

As will be shown later in this report, tests of a specific model with a boundary layer thinner than any of those mentioned in the preceding paragraph showed a decrease in pressure recovery resulting from the extension of the deflectors. Improvement resulted from the use of normal deflectors. It may be concluded, therefore, that for all boundary-layer thicknesses, the normal deflectors should be used but that the deflectors should be extended only when the boundary layer is as thick or thicker than boundary layer 2. In any specific application the controlling parameter to be used in applying the results of this investigation, insofar as the thickness of boundary layer is concerned, is the ratio of boundary-layer depth to the depth of the submerged entrance.

Boundary-layer control.— Boundary-layer-control tests were made with a suction slot located at various positions along the ramp as shown in figure 5. The effectiveness of the boundary-layer control was found to be best when the slot was located in the ramp near the inlet. The data obtained with the best slot (slot 4, fig. 5) are given in figures 26 and 27. These data show that, if the flow in the boundary-layer suction slot is about 20 percent of the flow into the submerged inlet, the best results are obtained. However, the improvement obtained by use of boundary-layer

control is no greater than is obtained by extending the deflectors. It is believed that the use of extended deflectors will show an over-all increase in airplane performance greater than for boundary-layer control. It is expected, however, that if the walls of the ramp have no divergence the effectiveness of the boundary-layer control will be much greater.

Drag.- No drag measurements were made in the general investigation in the small 1- by 1.5-foot wind channel. It is impossible to distinguish between the external and internal drag of a submerged inlet in the same manner as for an inlet in the leading edge of a wing or streamline body. Nearly all of the air which suffers a loss in momentum due to the presence of the submerged inlet flows into the entrance of the duct where that loss in momentum appears as a pressure loss. For the basic submerged duct it might be said that the external drag is a negative quantity, since there probably is an improvement of the flow behind the inlet because of the removal of the boundary layer.

It is expected, however, that the use of deflectors will result in some small external drag, but in view of the large increase in pressure recovery resulting from their use, it is believed they will result in a large net gain.

show?
for 2#03 program

[REDACTED]

Application to a Specific Design

As mentioned previously, the results of the general investigation were applied to a specific airplane design and tested on a 0.25-scale model in the 7- by 10-foot wind tunnel. The airplane used for this purpose is a high-speed fighter airplane powered with a Halford jet motor. From the results of the basic research, twin submerged entrances were designed to supply air to the Halford unit at an inlet-velocity ratio of 0.70 at an airspeed of 475 miles per hour at 15,000 feet altitude. The internal ducting was of constant area back to the twin entrances of the jet motor. Pressure losses in the ducting as determined from bench tests were found to be 10 percent of the dynamic pressure of the air flowing in the duct. Views of the submerged inlet are shown in figure 3, and a dimensioned sketch is given in figure 28.

The results of tests made for the basic submerged duct and for the inlet with normal deflectors are shown in figure 29. The use of the deflectors appreciably increased the pressure recovery at the high inlet-velocity ratios. Extending the deflectors had a deleterious effect on the pressure recovery. Since the boundary layer was very thin, these results substantiate the theory that the extended deflectors improve the pressure recovery only if the boundary layer is thick.

The results of tests in which the angle of attack was varied are shown in figure 30. It is interesting to note that the variation of pressure recovery with angle of attack is

[REDACTED]

p. 16

Should note that airplane
model had no serum, rate
in which, however, press theory
in difference can be used quantita-
tively. Shows need for
basic tests without initial rates
in order to compare theory
values for simple and applied
cases.

small. This represents a considerable improvement in flow characteristics over those obtained with an inlet in the leading edge of a wing or streamline body.

The estimated variation of critical Mach number with an inlet-velocity ratio based on measured pressures is given in figure 31. The decrease to a maximum M_{cr} of 0.79 at an inlet-velocity ratio of 0.95 from the value of 0.92 for the basic lip 6 represents the effect of the addition of the incremental velocity over the fuselage. The critical speed of the submerged inlet is much greater than that of other basic parts of the aircraft. The lip used was given approximately 2° of down incidence.

It may be concluded that the application of the results of the general investigation to a specific design presents no additional problems. It is considered, however, that the use of deflectors on the submerged duct for this design was made even more necessary because the duct was located in a curved surface. The negative incidence of the lip necessary for the attainment of high-critical speed was greater than for the lips tested in the general research because the surface in which the submerged duct was placed had appreciable curvature in the stream direction.

Data for Use by a Designer

From the preceding discussion of the research the following summary may be given:

1. Ramp design

- (a) The use of divergent walls for the ramp improves the pressure recovery to such magnitude as to make them mandatory for all installations. The curved divergence shows the best characteristics.
- (b) The ramp angle may be varied up to 10° . For a 10° ramp the pressure losses are slightly greater than for lesser ramp angles. If a 10° ramp is used, a lesser divergence should be used than for lesser ramp angles.

2. Lip design

- (a) Lip shape 6 is entirely satisfactory from the standpoint of critical-speed and internal-flow losses.
- (b) The effect of increasing the divergence is to increase the angle of attack of the lip at any given inlet-velocity ratio. This is believed due to increased divergence of the streamlines at the entrance resulting from increased pressure recovery.
- (c) The effect of increasing the ramp angle is to decrease the angle of attack of the lip.
- (d) For any ramp angle selected, similar critical-speed characteristics may be obtained by selecting the proper lip incidence.

*More study
on lips
at higher M*

(e) The use of a lip submerged below the surface into which the entrance is placed so that the lip contour becomes tangent to the surface at its maximum thickness appears to be most satisfactory.

3. Entrance aspect ratio

(a) Use of a square entrance in place of a rectangular one of aspect ratio 4.0 shows slightly greater pressure losses. It is more desirable to use an aspect ratio of about 4.0 for the entrance.

4. Boundary-layer thickness

(a) Increasing the boundary-layer thickness appreciably reduces the pressure recovery. This loss may be reduced by increasing the length of the deflectors along the top of the ramp walls.

5. Boundary-layer control

(a) The use of boundary-layer control does not appear practicable in view of the improvement in pressure recovery resulting from the use of divergent walls and deflectors.

In order to make the results of the research available in a more convenient form the following design data have been prepared for the entrance of figure 32, of aspect ratio 4.0 with 7° ramp, divergence 4 and lip 6:

1. Data showing the expected pressure recovery as a function of inlet-velocity ratio for any diffuser efficiency are presented in figure 33. Figure 34 presents similar data for the same entrance with normal deflectors. These data are for boundary layer 1. For boundary layers 2 and 3, data are presented for the basic ramp with extended deflectors in figures 35 and 36. These data may be considered to closely approximate the losses for ramp angles up to 10° .

2. Data showing the necessary alignment of the lip for ramp angles between 5° and 10° are shown in figure 37 together with the basic critical speed of the lip.

Design procedure.- The procedure necessary to estimate the characteristics of a submerged entrance designed for the aircraft of figure 38 is outlined below. This airplane is powered with a 3000-pound-thrust jet motor requiring 31 pounds of air per second at an airspeed of 550 miles per hour at 25,000 feet altitude. The air enters the jet motor at a velocity of 385 feet per second.

1. The selection of the inlet position ahead of the wing was made because of the thin boundary layer that exists on the fuselage and because the entrance is out of the velocity field of the wing. In general, it is believed good practice to locate submerged inlets in a region of relatively low velocity. The attainment of high-critical speed is made easier since the incremental velocities are small and the initial velocity of the air, which is slowed down on entering the duct, is less,

resulting in a less severe pressure gradient and a higher pressure recovery.

2. Twin ducts were used because of the large entrance area required which prohibited the use of a single inlet unless it was placed on the underside of the fuselage. It should be noted that for a twin-duct installation there is danger of flow instability occurring with consequent duct rumble if the inlet-velocity ratio in any flight condition falls below the value for maximum pressure recovery. This flight condition is found usually either in gliding flight with the motor throttled or off. This instability and consequent rumble may be eliminated by closing off one entrance for these flight conditions or by providing spoilers in the internal duct ahead of the juncture of the twin inlet ducting which are actuated when the throttle is closed. It may, also, be eliminated by providing air bleed in these flight conditions. The instability is found only for twin-duct installations and is entirely a function of the positive variation of pressure recovery with inlet-velocity ratio.

3. The boundary-layer thickness was calculated by the method of reference 3 and was found to be less in terms of the duct depth than the thinnest boundary layer tested.

4. It was decided that the entrance should have a 7° ramp. Curved divergence 4 and lip 6 with normal deflectors were used. Lip 6 was given 3° of down incidence.

5. An inlet-velocity ratio of 0.70 was selected to give

a critical speed of 0.85 for the basic lip.

6. This inlet-velocity ratio fixed the diffuser expansion at 1.9 to 1.0. The estimated diffuser efficiency was 85 percent.

7. The pressure recovery as a function of inlet-velocity ratio was estimated from figure 34. These data together with an estimate of the critical compressibility speed are given in figure 39.

It should be noted that, if a low inlet-velocity ratio (e.g., 0.5) is selected, there is a possibility that the pressure gradient ahead of the duct entrance may become so severe at high Mach numbers as to cause separation of the flow from the surface similar to that which occurs at low speed at inlet-velocity ratios less than 0.4. This will result in lower pressure recoveries than estimated. The use of fairly high inlet-velocity ratios is an essential characteristic of these submerged entrances. This, of course, intensifies the problem of diffuser design and makes essential the elimination of all bends and rapid expansions in the internal ducting. Fortunately, the submerged inlets may be so placed as to make this problem easier of solution than that for inlets in the leading edge of a wing or a streamline body.

CONCLUSIONS

As a result of the research conducted on the submerged air inlets the following conclusions may be drawn:

1. High-pressure recovery at the entrance at inlet-velocity

ratios less than unity of the duct may be obtained by diverging the walls of the ramp approaching the submerged entrance.

2. The pressure recovery at high inlet-velocity ratios is improved further by adding small deflectors to the top of the ramp walls.

3. Ramp angles up to 10° may be used without incurring excessive pressure losses.

4. Very high-critical-compressibility speed may be obtained by use of proper lip shape and incidence. *what is critical M.M.S. quite ?*

5. The existence of a thick boundary layer on the surface into which the inlet is placed will appreciably reduce the pressure recovery in terms of free-stream dynamic pressure. This loss may be eliminated to some extent by extending the deflectors forward to the leading edge of the entrance ramp.

6. The use of boundary-layer control is not as effective as the use of extended deflectors.

7. The variation of pressure recovery with angle of attack for a complete model is small, a characteristic which makes submerged inlets more desirable than wing leading-edge inlets.

8. Submerged inlets are well suited for use in supplying air to jet motors especially for those with axial flow compressors which use air at high velocity.

Ames Aeronautical Laboratory,
National Advisory Committee for Aeronautics,
Moffett Field, Calif., May 23, 1945.

Charles W. Frick

Charles W. Frick,
Aeronautical Engineer.

Wallace F. Davis

Wallace F. Davis,
Aeronautical Engineer.

Emmet A. Mossman

Emmet A. Mossman,
Mechanical Engineer.

Lauros Randall

Lauros Randall,
Aeronautical Engineer.

Approved:

Donald H. Wood

Donald H. Wood,
Aeronautical Engineer.

APPENDIX

Coefficients and Symbols

H	total pressure, pounds per square foot
p	static pressure, pounds per square foot
V	velocity, feet per second
ρ	air density, slugs per cubic foot
q	dynamic pressure ($\frac{1}{2}\rho V^2$), pounds per square foot
P	pressure coefficient $\left(\frac{P_L - P_o}{q_o}\right)$
ΔH	loss in total pressure ($H_L - H_o$), pounds per square foot
η_D	diffuser efficiency factor $\left(1 - \frac{\Delta H_D}{q_A}\right)$
M_{cr}	critical Mach number
α	angle of attack of model wing, degrees

Subscripts

A	station at the duct entrance
L	station at which the pressure measurements were made
o	free stream
av	average over duct section
D	diffuser

REFERENCES

- ✓ 1. Rogallo, F.M.: Internal-Flow Systems for Aircraft.
NACA Rep. No. 713, 1941.
- ✓ 2. von Kármán, Th.: Compressibility Effects in Aerodynamics.
Jour. Aero. Sci., vol. 8, no. 9, July 1941, pp. 337-356.
3. Jacobs, E.N., and Von Doenhoff, A.E.: Formulas for
Use in Boundary-Layer Calculations on Low-Drag Wings.
L-319 NACA ACR, Aug. 1941.

TABLE I.- ORDINATES FOR DIVERGENT RAMP WALLS

X/L \ Y/B	Divergence 0	Divergence 1	Divergence 2	Divergence 3	Divergence 4
0	0.50	0.500	0.500	0.5000	0.5000
.5	.50	.500	.500	.5000	.4930
.10	.50	.500	.500	.5000	.4670
.20	.50	.470	.458	.4470	.3870
.30	.50	.442	.415	.4000	.3100
.40	.50	.418	.373	.3500	.2420
.50	.50	.390	.333	.3050	.1950
.60	.50	.363	.290	.2550	.1550
.70	.50	.335	.250	.2080	.1200
.80	.50	.308	.205	.1580	.0750
.90	.50	.280	.165	.1100	.0575
1.00	.50	.250	.125	.0625	.0440

Note: Reference axes are shown on figure 6.

TABLE II(a).- LIP ORDINATES GIVEN IN INCHES

Sta- tion	Lip 1		Lip 2		Lip 3		Lip 4		Lip 5		Lip 6		Lip 7	
	Upper	Lower	Upper	Lower	Upper	Lower	Upper	Lower	Upper	Lower	Upper	Lower	Upper	Lower
0	-0.125	-0.125	-0.125	-0.125	-0.220	-0.220	-0.125	-0.125	-0.125	-0.125	-0.063	-0.063	-0.063	-0.063
.25	0	-.265	0	-.320	-.030	-.360	.065	-.310	.065	-.280	.100	-.275	.160	-.280
.50	0	-.296	0	-.380	0	-.390	.115	-.370	.115	-.350	.150	-.350	.210	-.360
.75	0	-.336	0	-.415	0	-.421	.125	-.410	.125	-.395	.175	-.410	.230	-.410
1.00	0	-.367	0	-.440	0	-.451	.120	-.440	.120	-.440	.187	-.440	.250	-.440
1.50	0	-.428	0	-.501	0	-.512	.110	-.500	.110	-.501	.187	-.505	.240	-.505
2.00	0	-.488	0	-.563	0	-.574	.100	-.560	.100	-.562	.175	-.570	.220	-.570
2.50	0	-.550	0	-.624	0	-.635	.085	-.622	.085	-.623	.150	-.631	.180	-.631
3.00	0	-.611	0	-.685	0	-.696	.060	-.683	.060	-.685	.120	-.692	.150	-.693
3.50	0	-.673	0	-.746	0	-.757	.030	-.745	.030	-.746	.085	-.753	.110	-.754
4.00	0	-.734	0	-.807	0	-.818	0	-.806	0	-.808	.055	-.815	.060	-.815
4.50	0	-.795	0	-.869	0	-.880	0	-.867	0	-.869	0	-.877	0	-.877
	L.E. radius: 0.125		L.E. radius: 0.125		L.E. radius: 0.125		L.E. radius: 0.125		L.E. radius: 0.075		L.E. radius: 0.125		L.E. radius: 0.1875	

Note: For location of reference line, see figure 15(b).

TABLE II(b).- ORDINATES FOR SUBMERGED
LIP 6 IN INCHES

Station	Outer surface	Inner surface
0	-0.240	-0.240
.25	-.087	-.462
.50	-.037	-.537
.75	-.012	-.597
1.00	0	-.627
1.50	0	-.692
2.00	0	-.757
2.50	0	-.819
3.00	0	-.879
3.50	0	-.940
4.00	0	-1.002
4.50	0	-1.064

Leading-edge radius = 0.125

Note: For location of reference line,
see figure 15(b).

FIGURE LEGENDS

- Figure 1.- The 1- by 1½-foot wind channel as arranged for submerged-duct-entrance tests.
- Figure 2.- Sketches of submerged duct entrances.
- Figure 3.- Submerged-duct installation on a 0.25-scale model of a fighter airplane. (a) View with normal deflectors. (b) View without deflectors.
- Figure 4.- The location of the pressure-survey tubes in the entrance of the submerged duct entry.
- Figure 5.- Sectional view of submerged duct entry showing boundary-layer-control slots tested.
- Figure 6.- The divergent ramp walls tested with various ramp angles.
- Figure 7.- The variation of dynamic-pressure recovery after diffusion with inlet-velocity ratio for diverging ramp walls.
- Figure 8.- Pressure losses at the center of the submerged duct entrance with various diverging ramp walls.
- Figure 9.- Pressure losses at the sides of the submerged duct entrance with various diverging ramp walls.
- Figure 10.- Deflectors tested with submerged duct.
- Figure 11.- The variation of dynamic-pressure recovery after diffusion with inlet-velocity ratio for various deflectors.
- Figure 12.- The variation of dynamic-pressure recovery after diffusion with inlet-velocity ratio for various ramp angles and no divergence.
- Figure 13.- The variation of dynamic-pressure recovery after diffusion with inlet-velocity ratio for various ramp angles and diverging walls.
- Figure 14.- The pressure gradient along the ramp floor for various ramp angles.
- Figure 15.- Lip shapes tested with the submerged duct. (a) Normal lips.
- Figure 15.- Lip shapes tested with the submerged duct. (b) Submerged lip.

Figure 16.- Pressure-coefficient distribution for various inlet-velocity ratios with lip 6 at zero incidence for a 7° ramp angle.

Figure 17.- Pressure-coefficient distribution for various inlet-velocity ratios with lip 6 at -3° incidence.

Figure 18.- The variation of critical Mach number with inlet-velocity ratio for lip 6 at 0° and -3° incidence.

Figure 19.- Pressure-coefficient distribution for various inlet-velocity ratios with lip 6 at zero incidence for a 5° ramp angle.

Figure 20.- Pressure-coefficient distribution for various inlet-velocity ratios with lip 6 at zero incidence for a 10° ramp angle.

Figure 21.- The variation of dynamic-pressure recovery after diffusion with inlet-velocity ratio for two entrance shapes.

Figure 22.- Variation of dynamic-pressure recovery after diffusion with inlet-velocity ratio for two submerged-duct-entrance shapes for boundary layer 2.

Figure 23.- Boundary layers for which submerged-duct tests were made.


Figure 24.- The variation of dynamic-pressure recovery after diffusion with inlet-velocity ratio for three boundary-layer thicknesses.

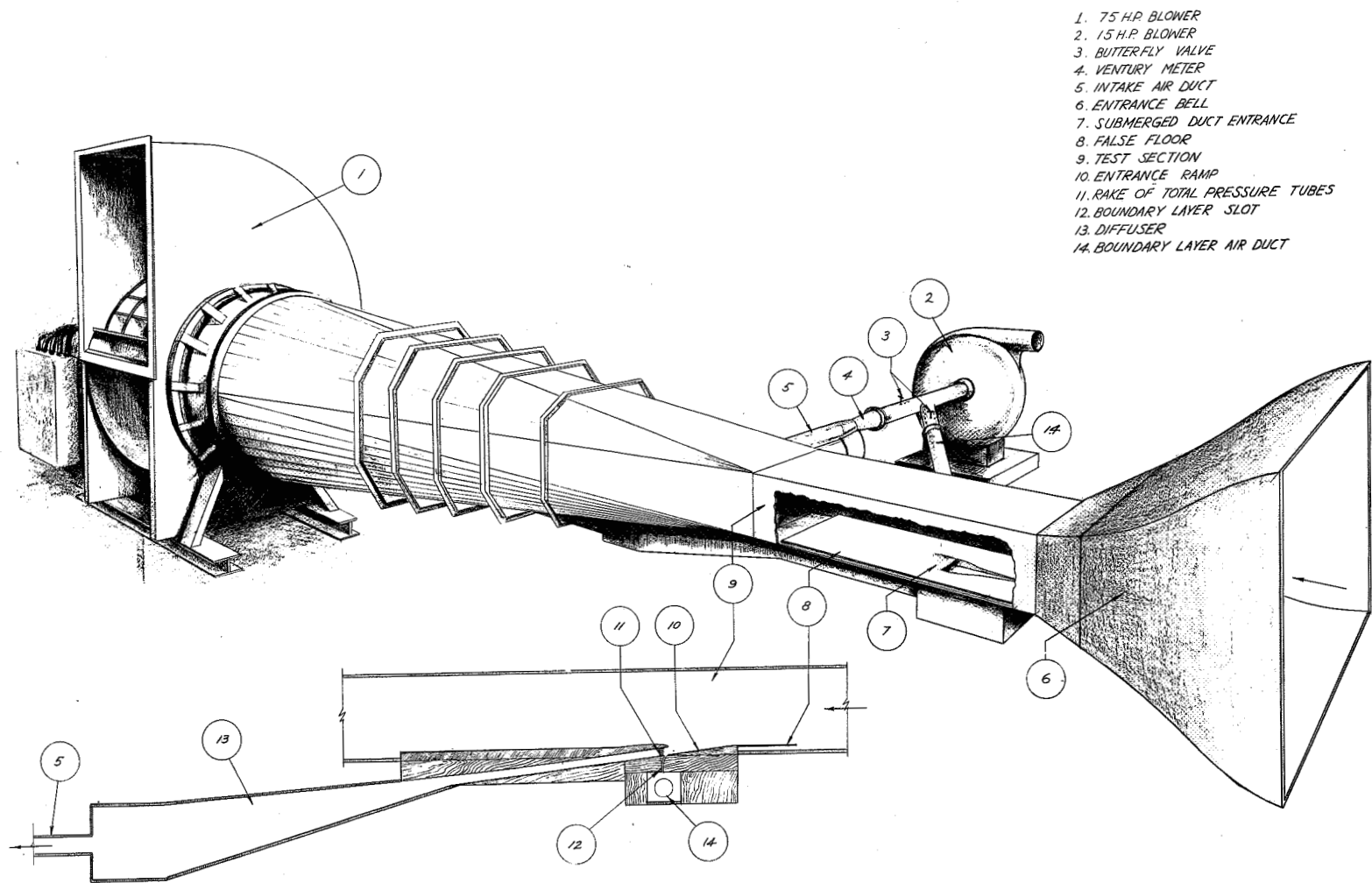
Figure 25.- The variation of dynamic-pressure recovery after diffusion with inlet-velocity ratio for various boundary layers and deflectors.

Figure 26.- The variation of dynamic-pressure recovery after diffusion with quantity of flow through the boundary-layer slot for various inlet-velocity ratios and boundary layers.

Figure 27.- The variation of dynamic-pressure recovery after diffusion with inlet-velocity ratio for 20 percent of the intake air drawn into the boundary layer.

Figure 28.- Sketch of the submerged-duct entrance installed on the 0.25-scale model of a fighter airplane. No deflectors.

- Figure 29.- Variation of dynamic-pressure recovery with inlet-velocity ratio for various deflector configurations, Submerged-duct installation on a 0.25-scale model of a fighter airplane.
- Figure 30.- Dynamic-pressure recovery of the 0.25-scale model of a fighter airplane with submerged-duct entries.
- Figure 31.- Variation of critical Mach number with inlet-velocity ratio for the submerged-duct installation on the 0.25-scale model of a fighter airplane. Matched operating conditions.
- Figure 32.- Sketch of submerged-duct entry for which design data are given.
- Figure 33.- The variation of dynamic-pressure recovery after diffusion with inlet-velocity ratio for various diffuser efficiency factors. No deflectors.
- Figure 34.- The variation of dynamic-pressure recovery after diffusion with inlet-velocity ratio for various diffuser efficiency factors. Normal deflectors.
- Figure 35.- The variation of dynamic-pressure recovery after diffusion with inlet-velocity ratio for various diffuser efficiency factors. Extended deflectors and boundary layer 2.
- Figure 36.- The variation of dynamic-pressure recovery after diffusion with inlet-velocity ratio for various diffuser efficiency factors. Extended deflectors and boundary layer 3.
- Figure 37.- The variation of the angle of lip 6 with ramp angle for high-critical speeds.
- Figure 38.- Three-view drawing of a high-speed jet fighter design.
- Figure 39.- The variation of dynamic-pressure recovery after diffusion and critical Mach number with inlet-velocity ratio for a submerged duct entrance on a typical fighter airplane.
- 



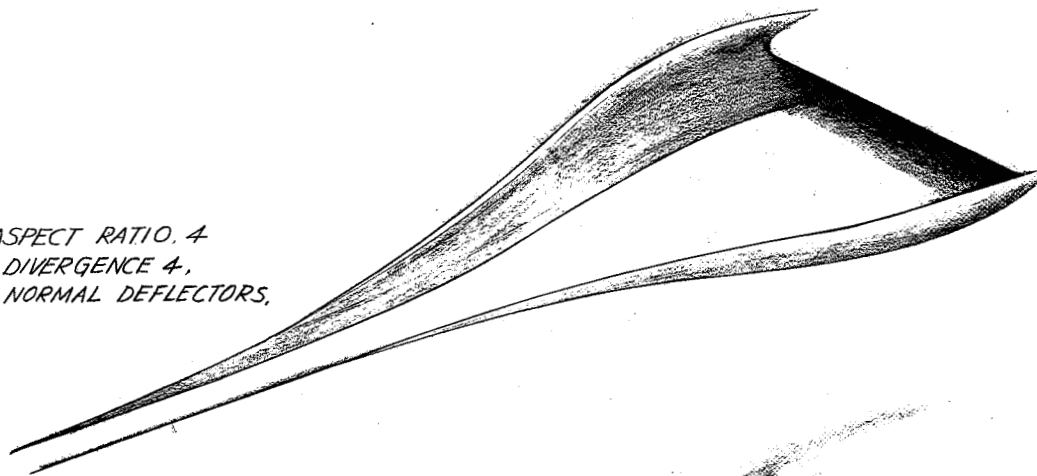
1. 75 H.P. BLOWER
2. 15 H.P. BLOWER
3. BUTTERFLY VALVE
4. VENTURY METER
5. INTAKE AIR DUCT
6. ENTRANCE BELL
7. SUBMERGED DUCT ENTRANCE
8. FALSE FLOOR
9. TEST SECTION
10. ENTRANCE RAMP
11. RAKE OF TOTAL PRESSURE TUBES
12. BOUNDARY LAYER SLOT
13. DIFFUSER
14. BOUNDARY LAYER AIR DUCT

NACA
A-7935
5-22-45

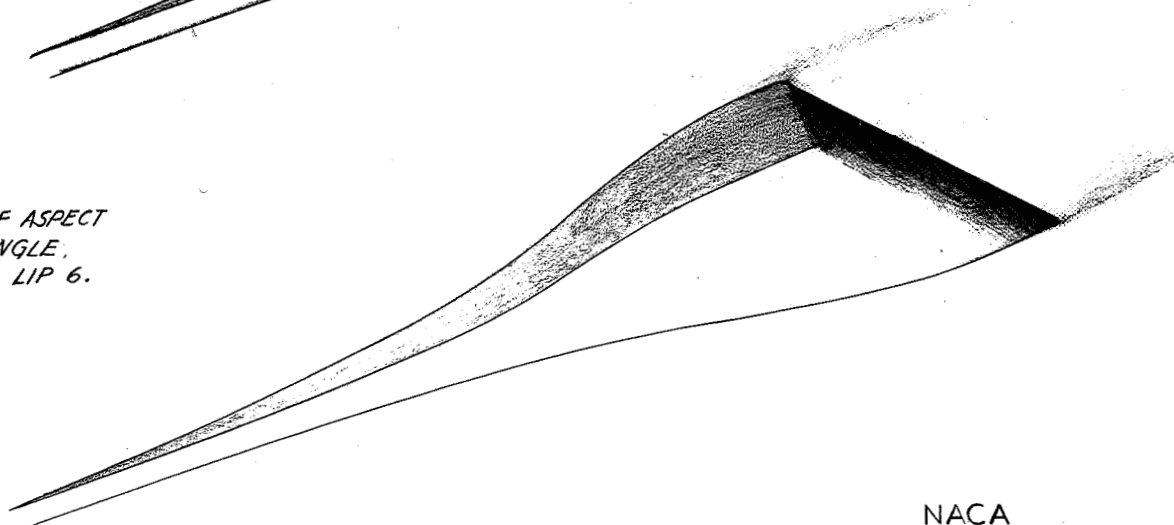
L.M. MASTIN
5-22-45

FIGURE 1. 1-BY 1½- FOOT WIND CHANNEL AS ARRANGED FOR SUBMERGED-DUCT-ENTRANCE TESTS.

a) DUCT ENTRANCE OF ASPECT RATIO 4
WITH 7° RAMP ANGLE DIVERGENCE 4,
SUBMERGED LIP, AND NORMAL DEFLECTORS.



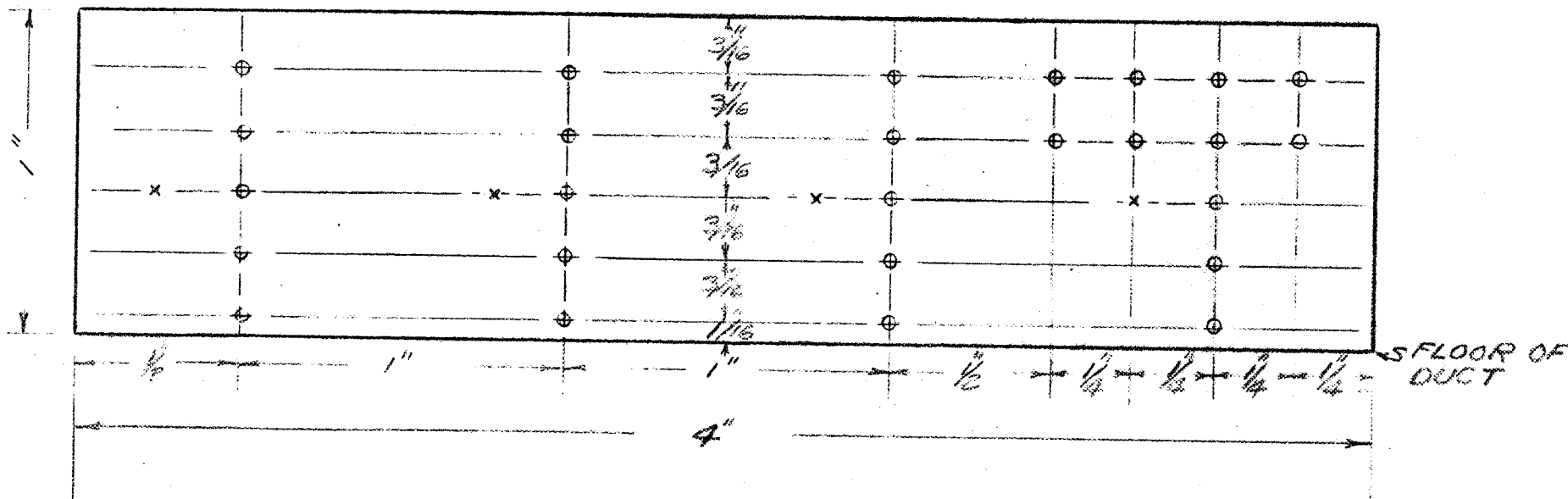
b) DUCT ENTRANCE OF ASPECT
RATIO 4, 7° RAMP ANGLE,
DIVERGENCE 4, AND LIP 6.



NACA
A-7936 L.M. MASTIN
5-20-45 5-20-45

FIGURE 2. SKETCHES OF SUBMERGED DUCT ENTRANCES.

- TOTAL PRESSURE TUBE
- x STATIC PRESSURE TUBE



SCALE 2" = 1"

NOTE
TUBES WERE LOCATED 1" AFT
OF LEADING EDGE OF LIP

FIGURE 4.- THE LOCATION OF THE PRESSURE-SURVEY TUBES IN THE ENTRANCE OF THE SUBMERGED DUCT ENTRY.

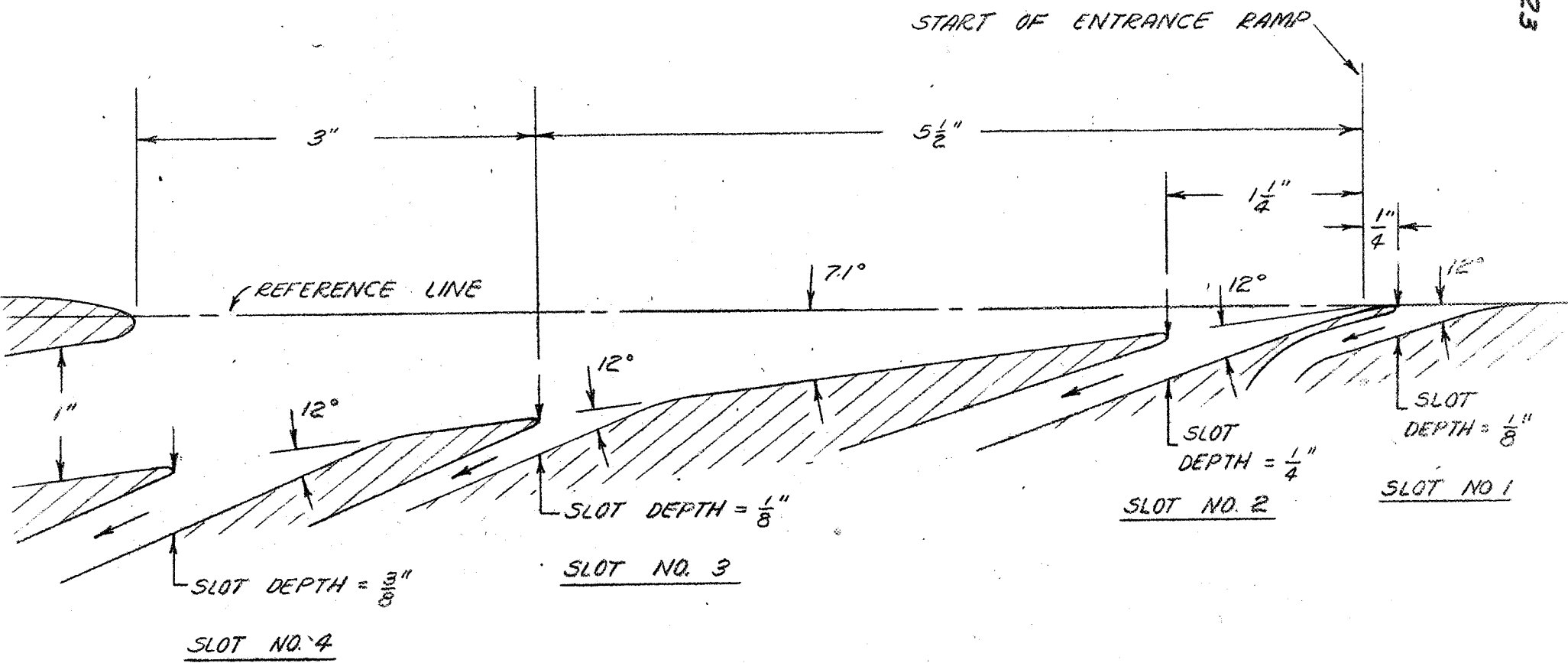


FIGURE 5.- SECTIONAL VIEW OF SUBMERGED DUCT ENTRY SHOWING BOUNDARY LAYER CONTROL SLOTS TESTED

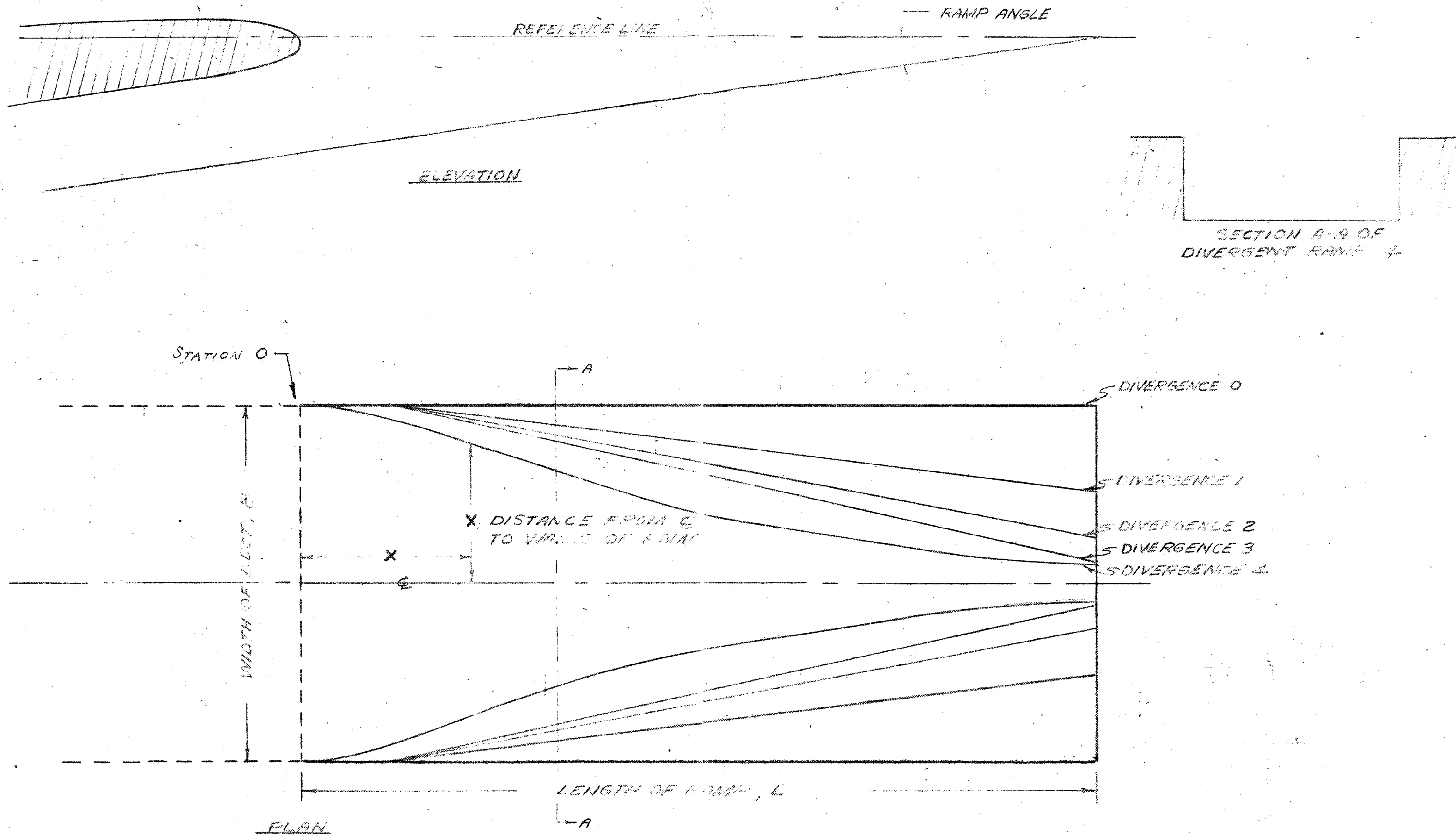


FIG. 6 - THE DIVERGENT RAMP ANGLES TESTED WITH VARIOUS RAMP ANGLES

DYNAMIC PRESSURE RECOVERY P/P_0

θ RAMP ANGLE
BOUNDARY LAYER
LIFE

SYMBOL	DIVERGENCE
+	0
□	1
△	2
◇	3
○	4

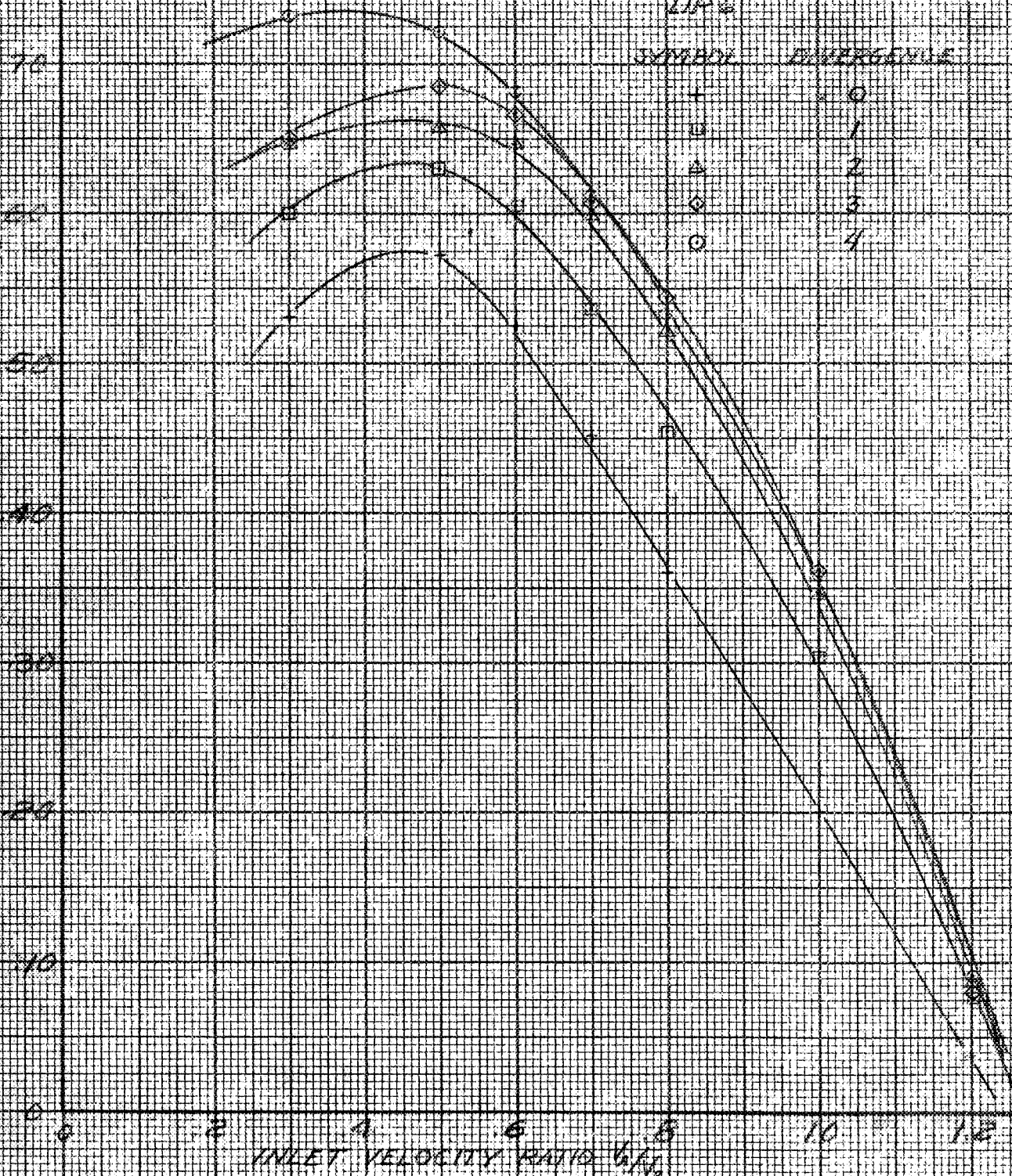


FIGURE 7.- THE VARIATION OF DYNAMIC PRESSURE RECOVERY AFTER DIFFUSION WITH INLET-VELOCITY RATIO FOR DIVERGING RAMP WALLS

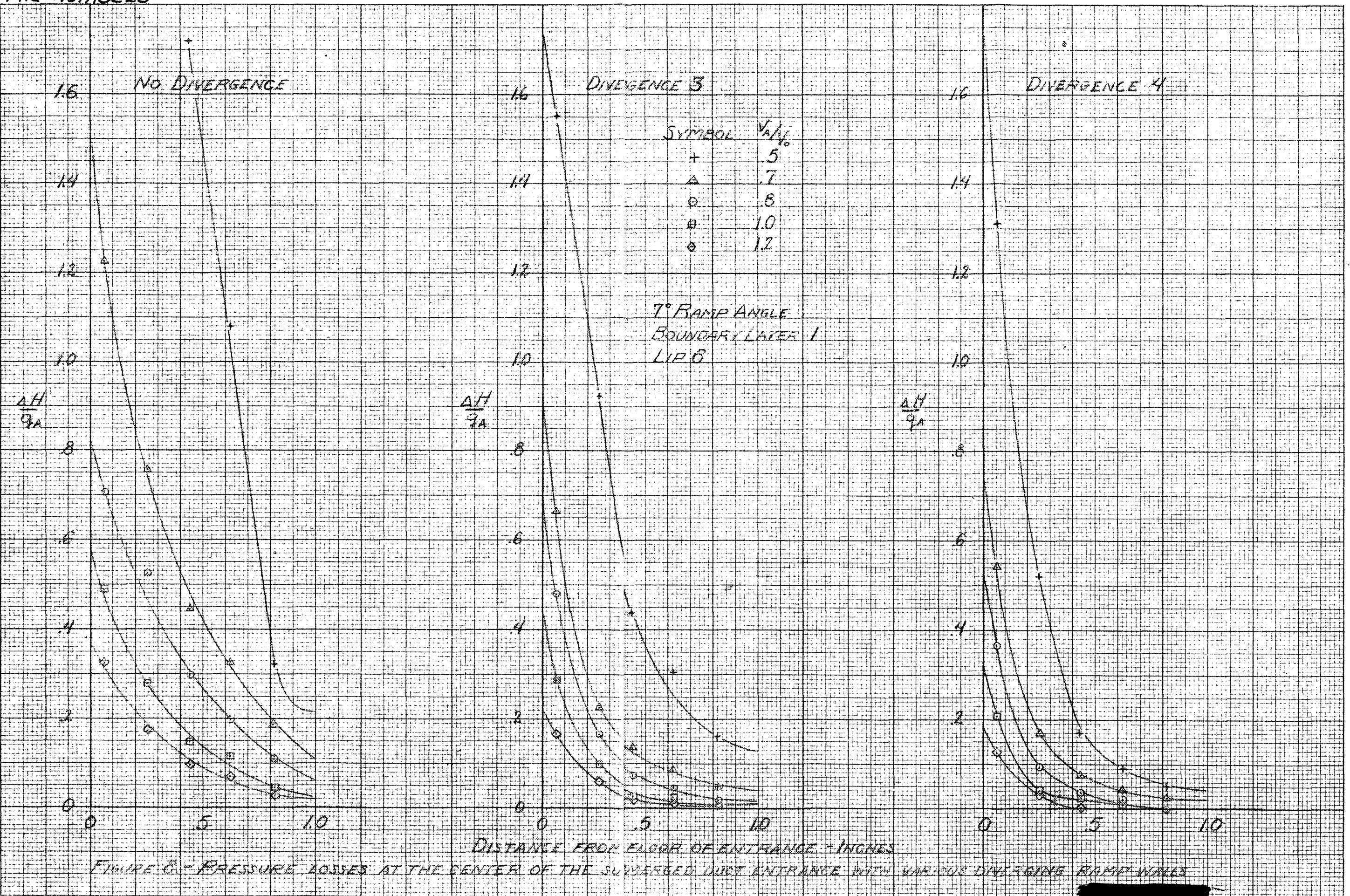


FIGURE 6 - PRESSURE LOSSES AT THE CENTER OF THE SUBMERGED JET ENTRANCE WITH VARIOUS DIVERGING RAMP WALLS

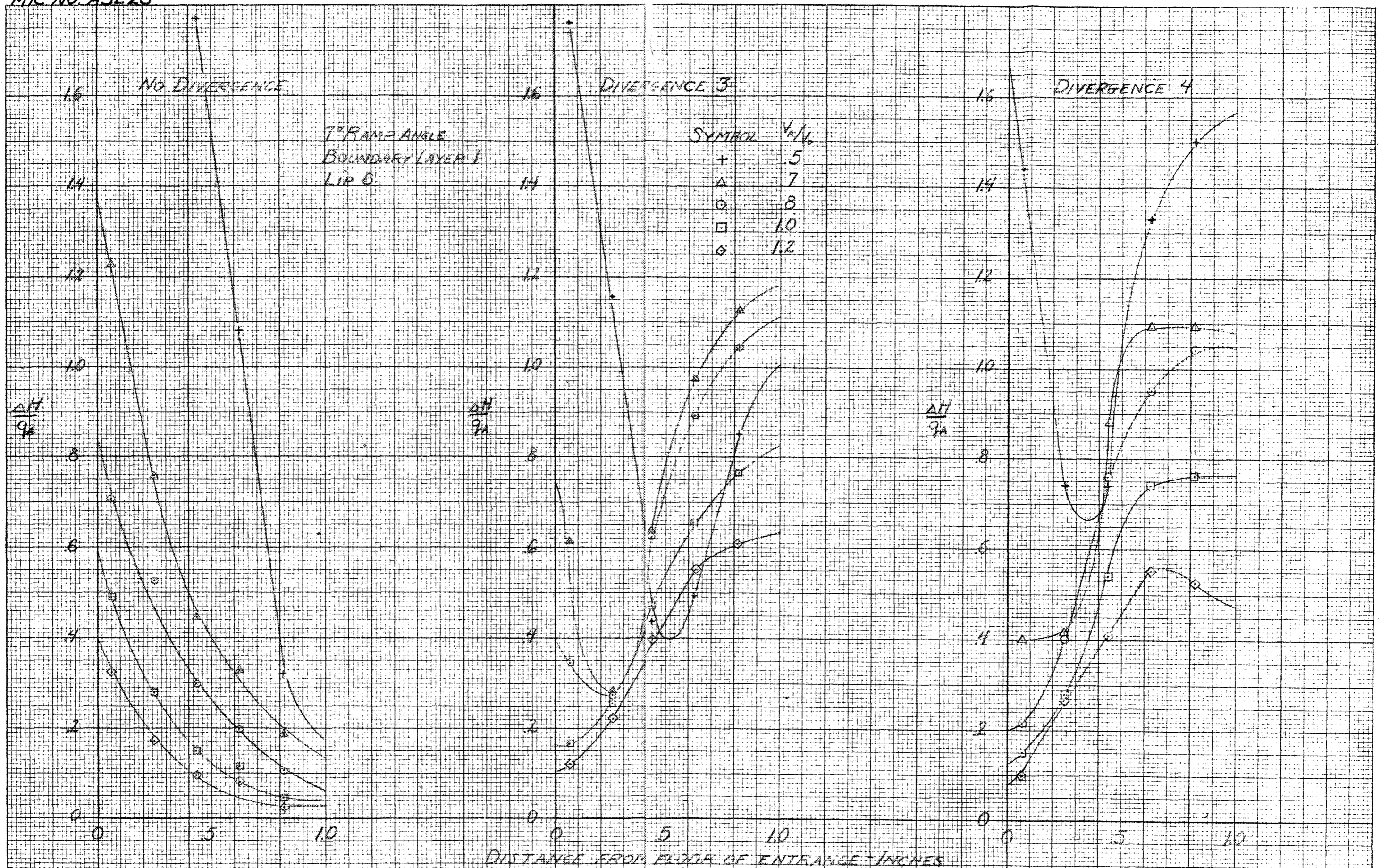
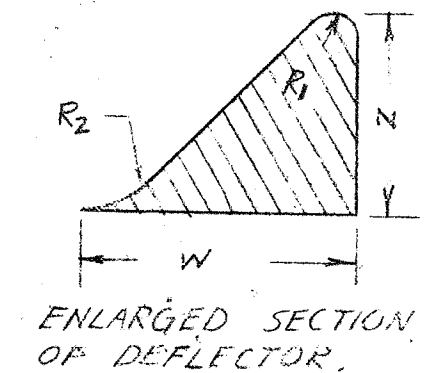
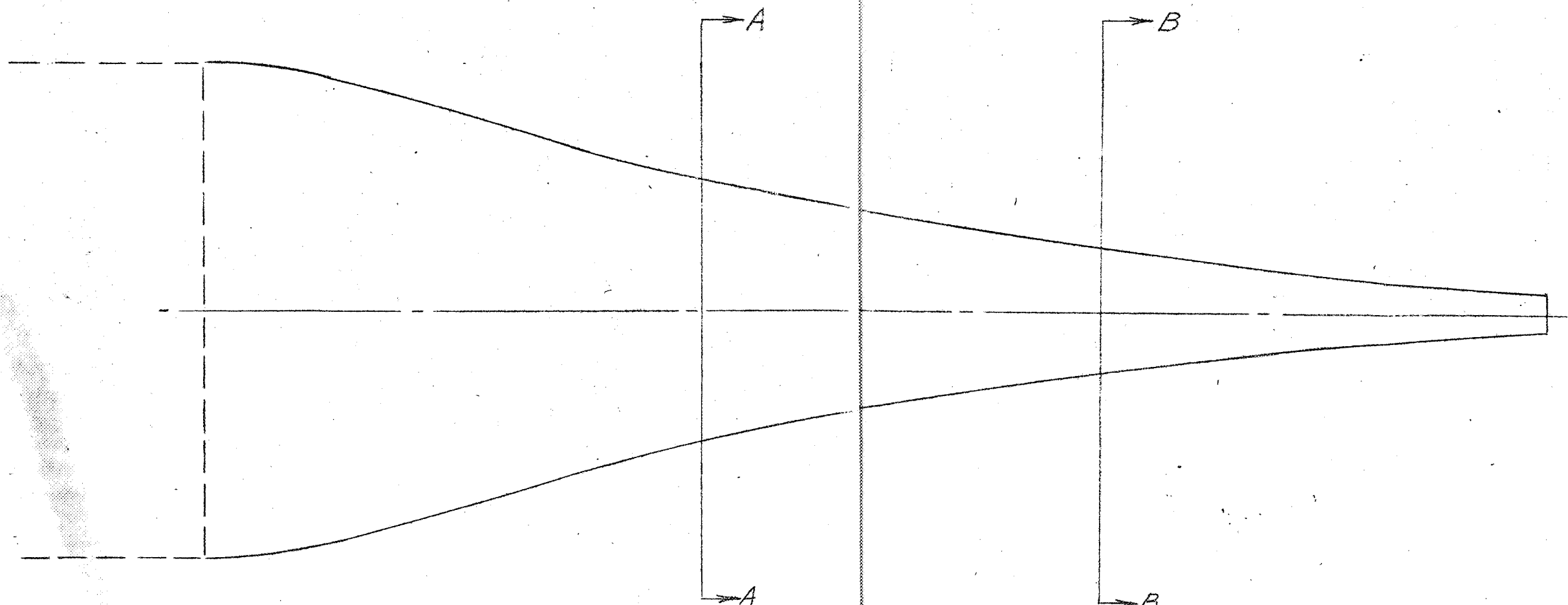
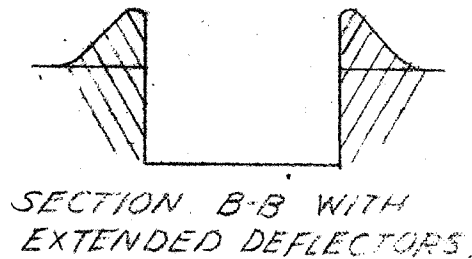
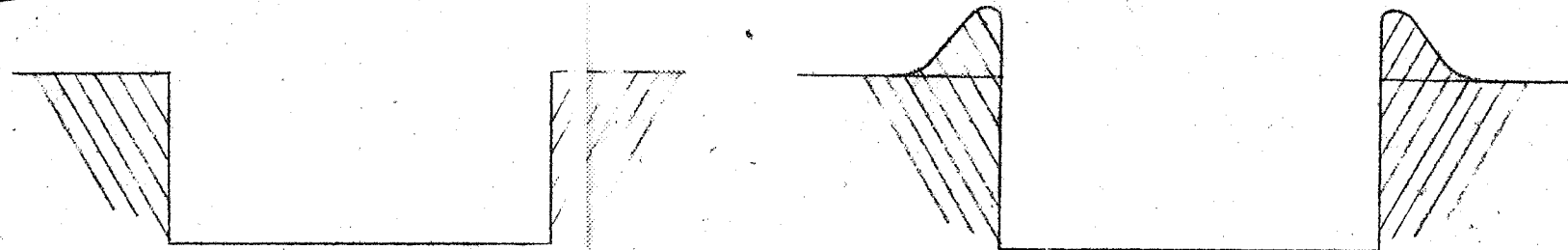
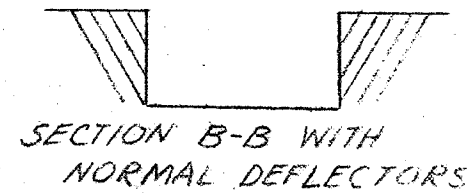
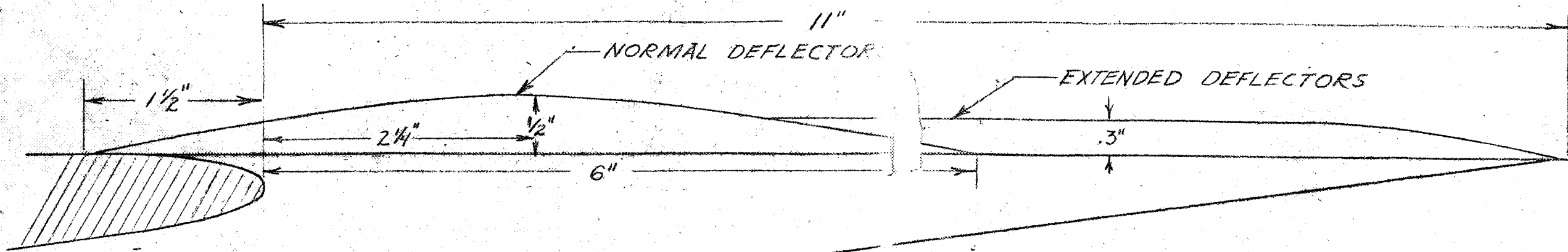


FIGURE 9. - PRESSURE LOSSES AT THE SIDES OF THE SUBMERGED DUCT ENTRANCE WITH VARIOUS DIVERGENCE FROM PARALLEL

MR NO. A5E23



$$W = 1.5z$$

$$R_1 = .5z$$

$$R_2 = .15z$$

FIGURE 10.— DEFLECTORS TESTED WITH SUBMERGED DUCT.

DYNAMIC PRESSURE RECOVERY (%)

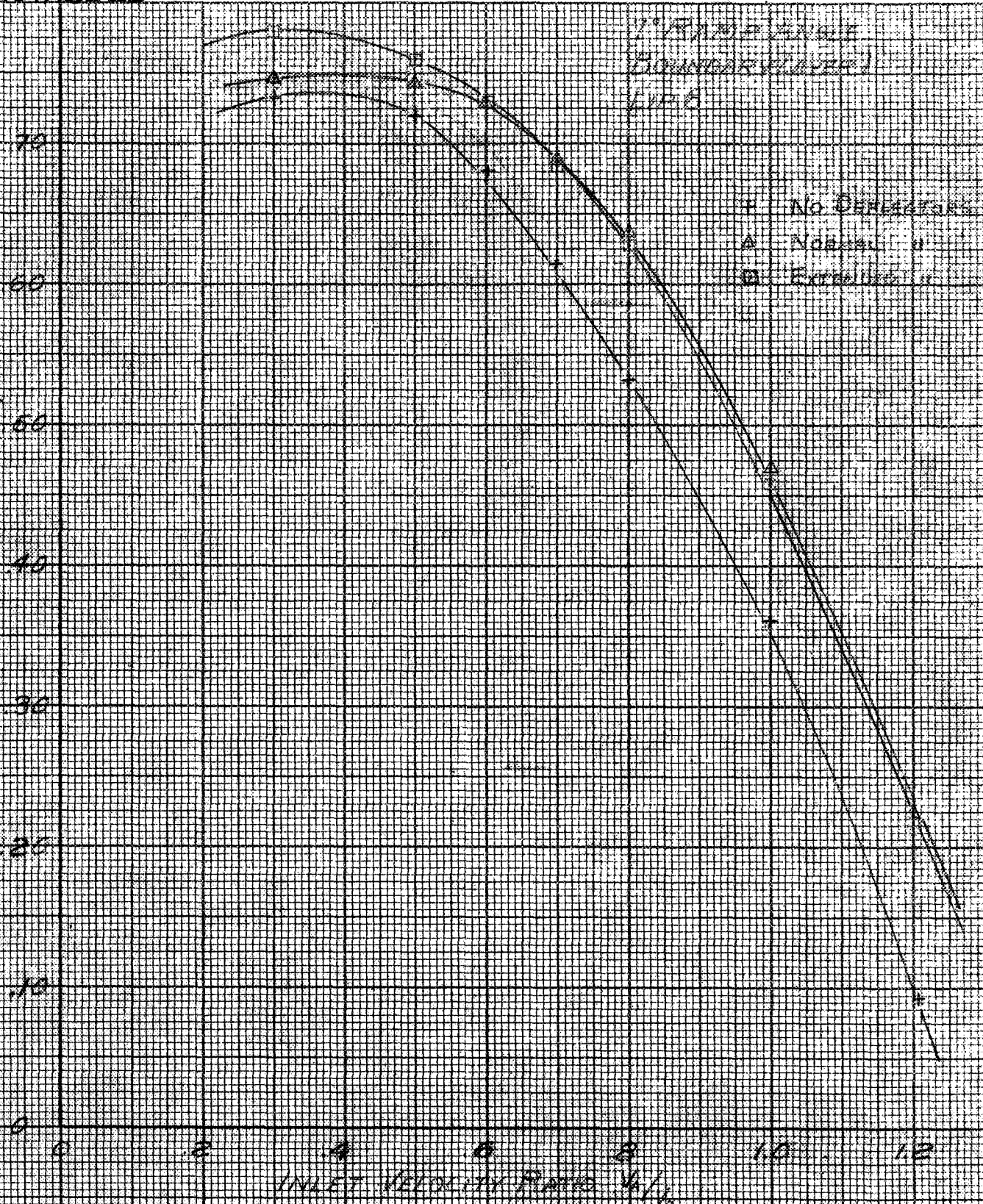


FIGURE 11. THE VARIATION OF DYNAMIC PRESSURE RECOVERY AFTER DIFFUSION WITH INLET VELOCITY RATIO FOR VARIOUS DEFLECTORS.

89-177 89710

ENGINE DESIGNER CO NO 742 B

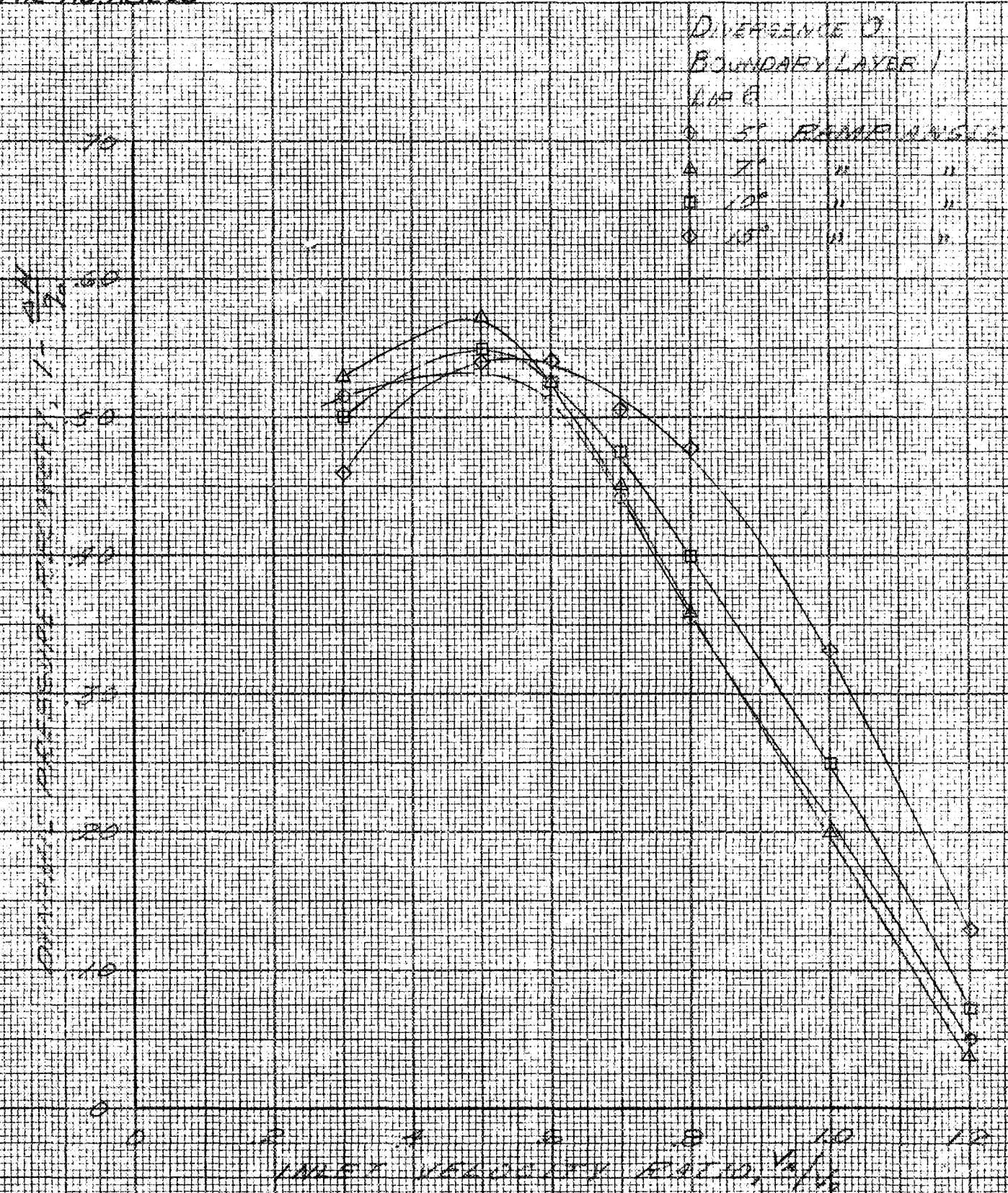


FIGURE 12. THE VARIATION OF DYNAMIC PRESSURE RECOVERY AFTER DIFFUSION WITH INLET-VELOCITY RATIO FOR VARIOUS FLAME ANGLES AND NO DIVERGENCE

A 2 U M 0 2 1 0 1 0

DYNAMIC PRESSURE RECOVERY, $\frac{P}{P_0}$

DIVERGENCE 2
 BOUNDARY LAYER 1
 LIA 6
 ○ 5° BOUND ANGLE
 ▲ 7° " " " "
 ⊙ 10° " " " "
 ⊠ 15° " " " "

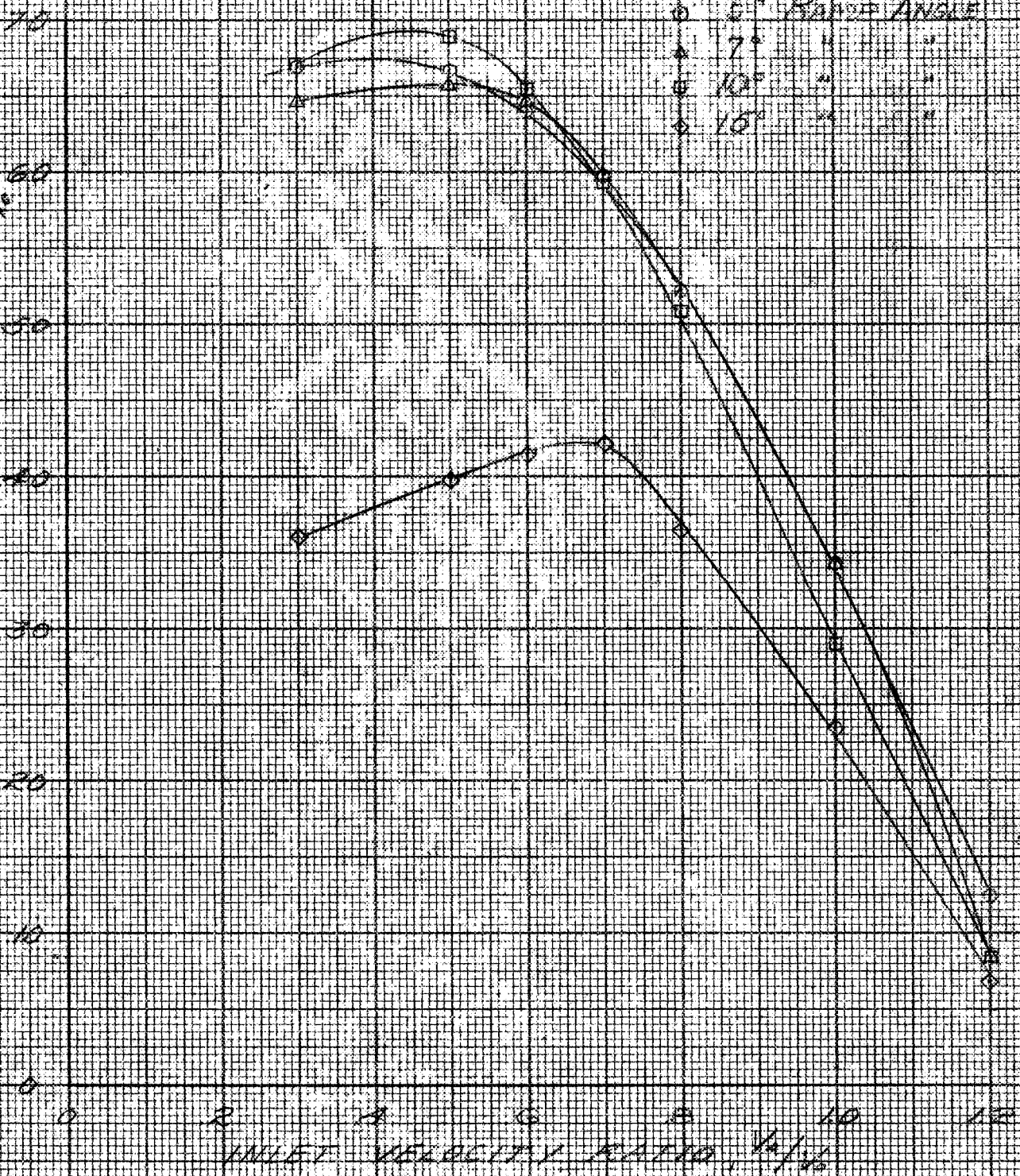


FIGURE 13. THE VARIATION OF DYNAMIC PRESSURE RECOVERY AFTER DIFFUSION WITH INLET-VELOCITY RATIO FOR VARIOUS RAMP ANGLES AND DIVERGENCE WALLS

- $V_{90} = 7$
- FREE WIND
 - △ 5° RAMP, DIVERGENCE 4
 - 7° RAMP, DIVERGENCE 4
 - ◇ 10° RAMP, DIVERGENCE 2
 - ▽ 10° RAMP, DIVERGENCE 3

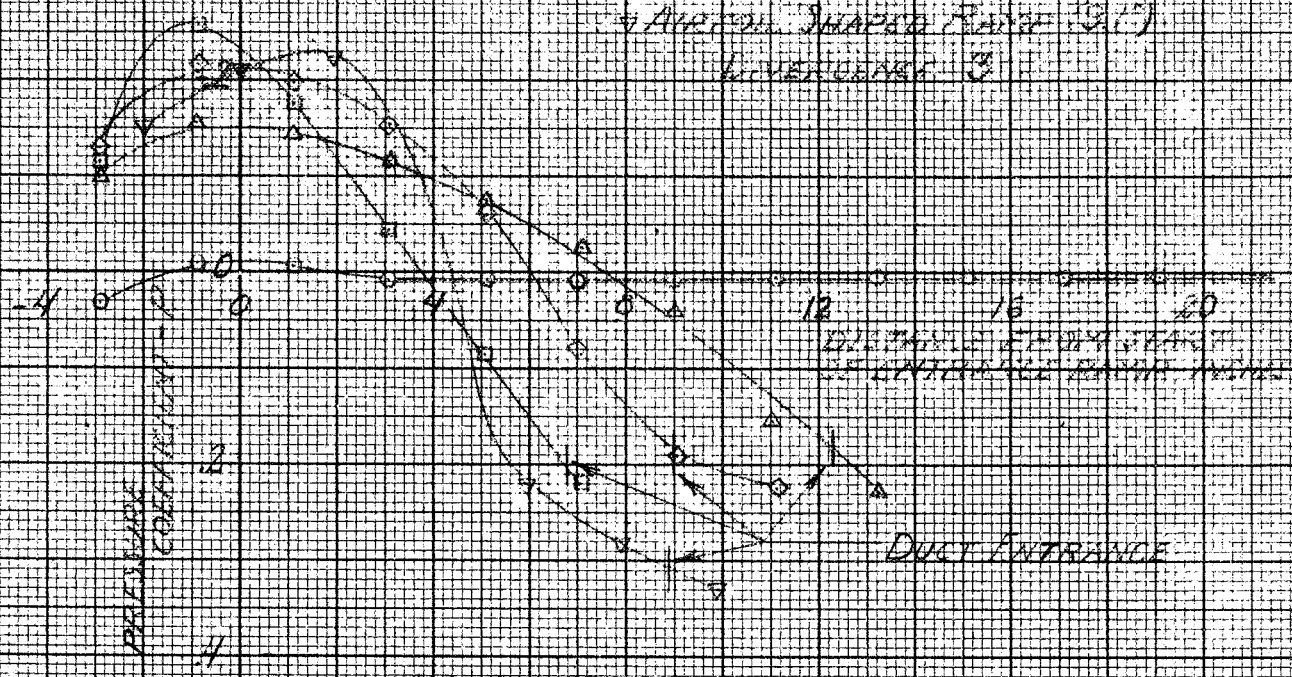
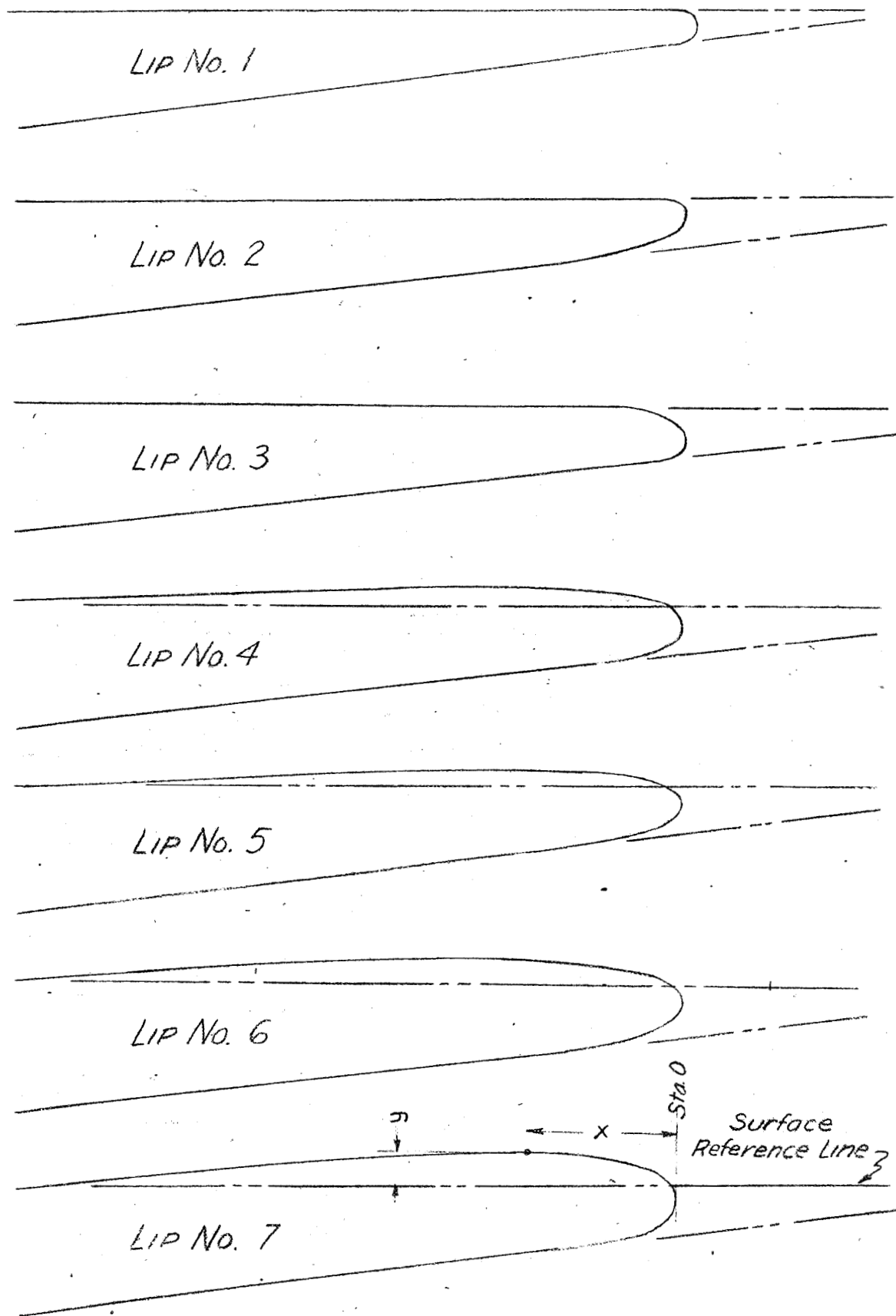


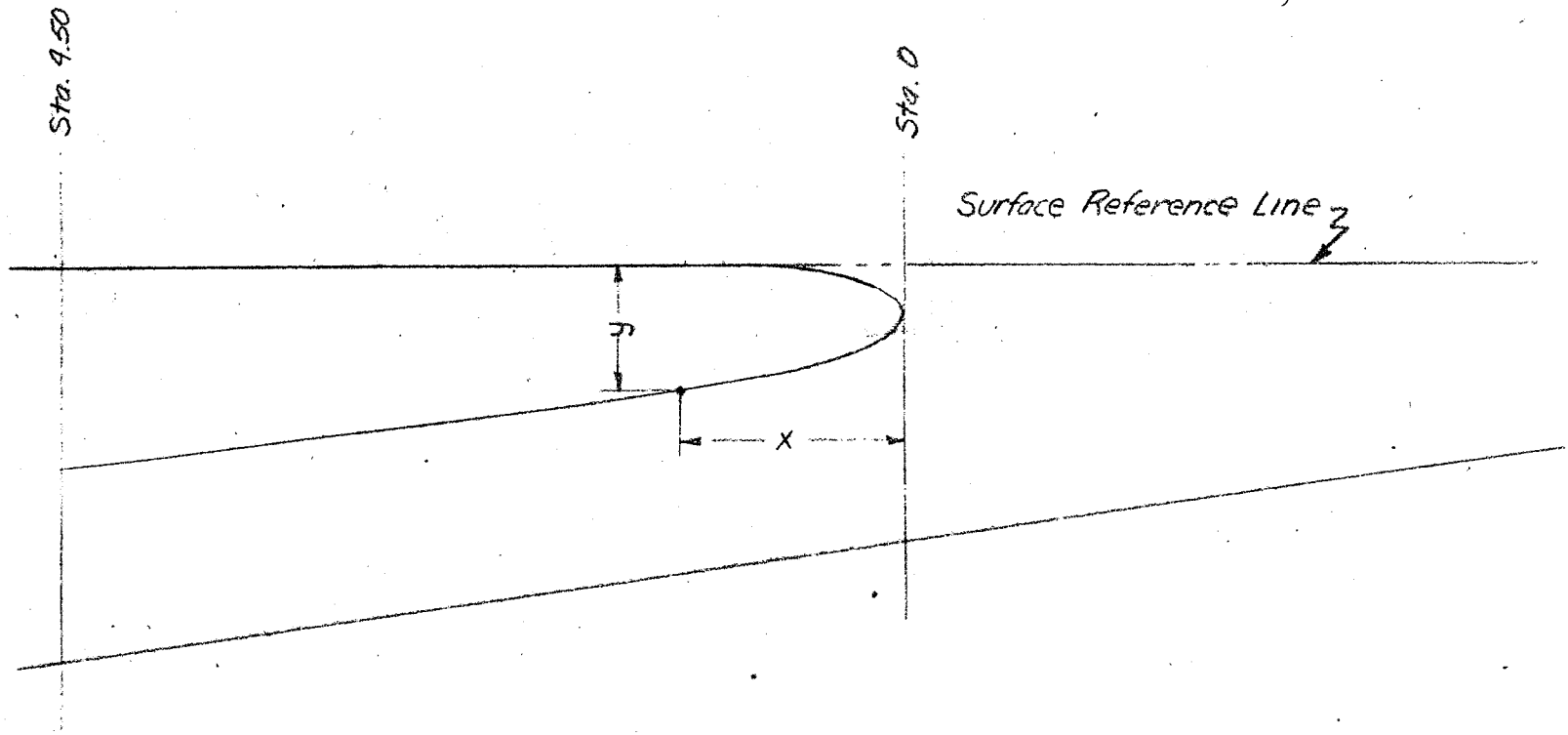
FIGURE 14 - THE PRESSURE GRADIENT ALONG THE RAMP FLIPS FOR VARIOUS RAMP ANGLES

MADE IN U. S. A.
 Plotting 1 x 10 in.
 10 x 10 to file # 10 x 10 in. plot lines measured.
 KENNER & PETER CO., N. Y. NO. 388-11



(a) NORMAL LIPS.

FIGURE 15.-LIP SHAPES TESTED WITH THE SUBMERGED DUCT.



(b.) SUBMERGED LIP
 FIGURE 15.- LIP SHAPES TESTED WITH THE SUBMERGED DUCT.

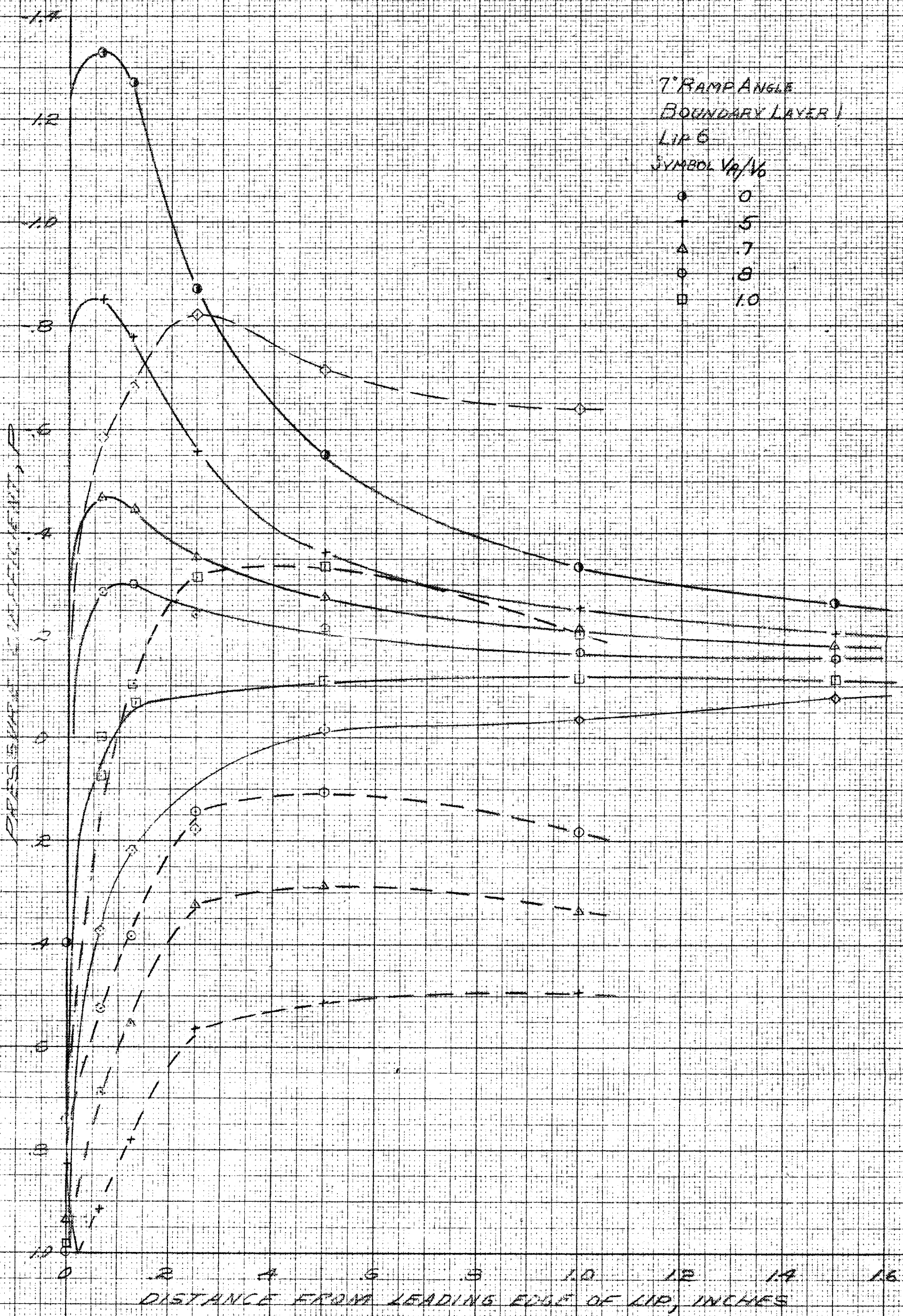


FIGURE 16 - PRESSURE-COEFFICIENT DISTRIBUTION FOR VARIOUS INLET-VELOCITY RATIOS WITH LIP 6 AT ZERO INCIDENCE FOR A 7° RAMP ANGLE

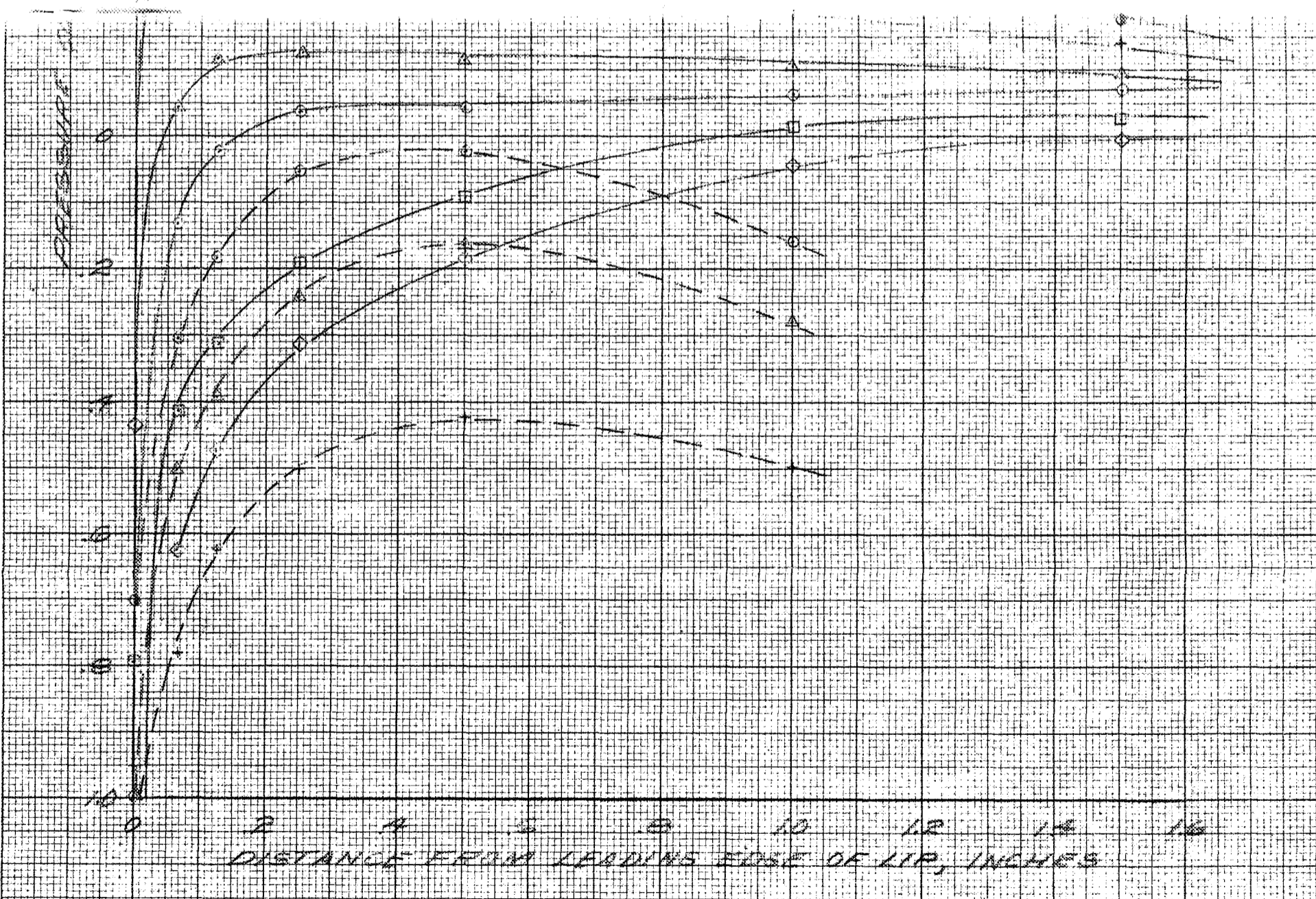
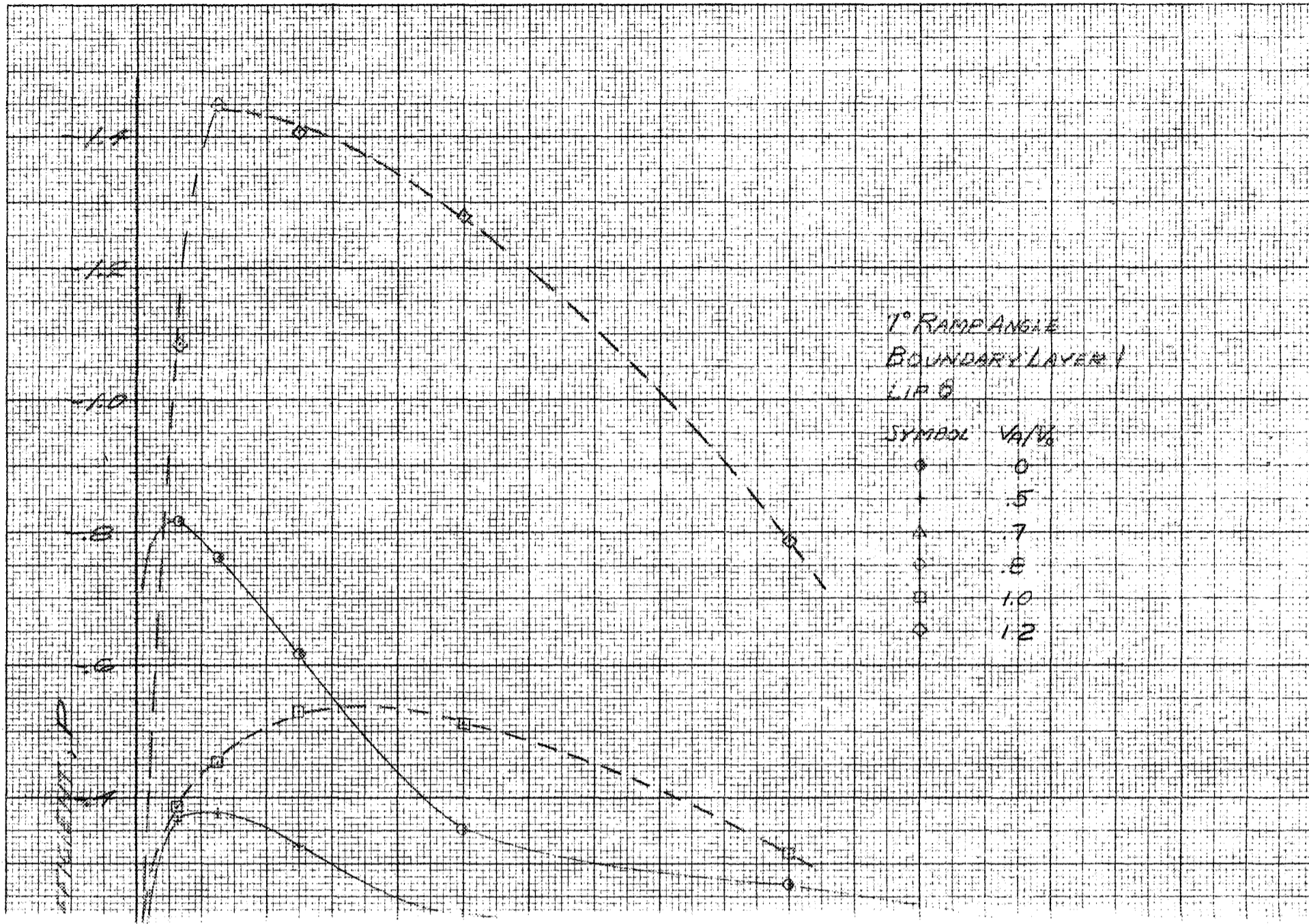


FIGURE 17 - PRESSURE-COEFFICIENT DISTRIBUTION FOR VARIOUS INLET-VELOCITY RATIOS WITH LIP 6 AT 3° INCIDENCE

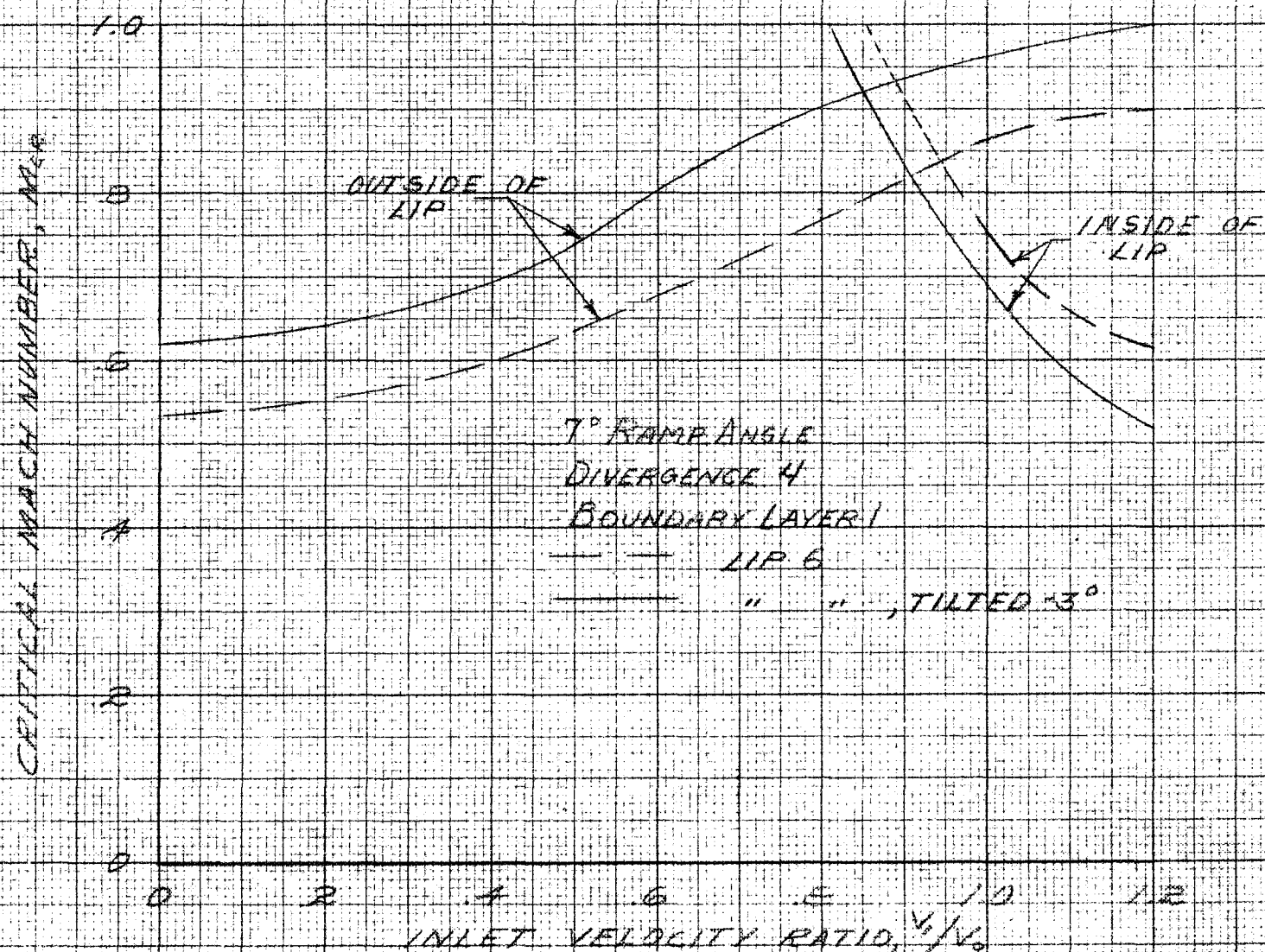


FIGURE 13 - THE VARIATION OF CRITICAL MACH NUMBER WITH INLET VELOCITY RATIO FOR LIP 6 AT 0° AND 3° INCIDENCE

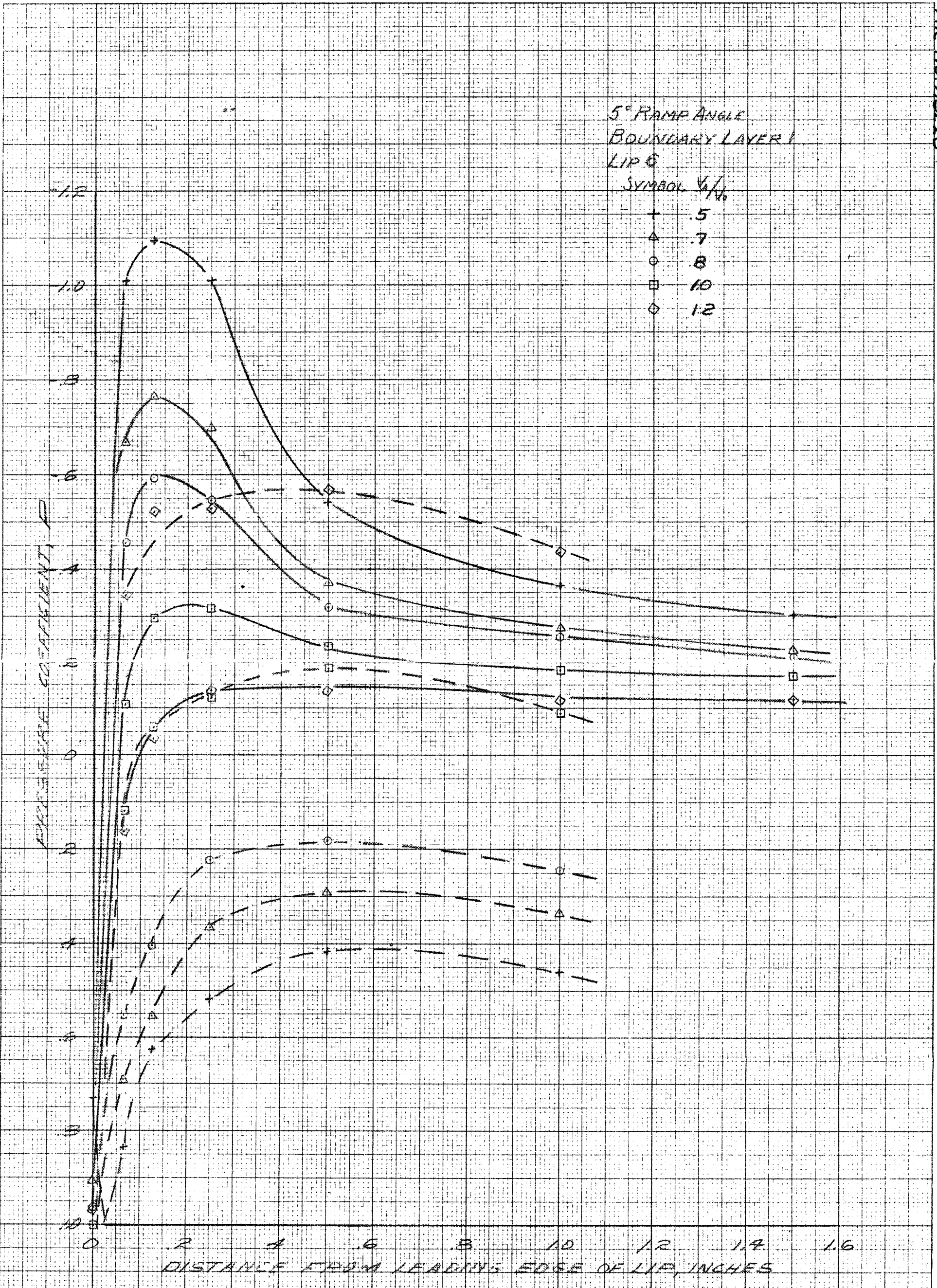


FIGURE 19.- PRESSURE-COEFFICIENT DISTRIBUTION FOR VARIOUS INLET-VELOCITY RATIOS WITH LIP 6 AT ZERO INCIDENCE FOR A 5° RAMP ANGLE

10° RAMP ANGLE
 BOUNDARY LAYER I
 LIP 6

SYMBOL	V_1/V_0
○	0
+	.5
△	.7
◇	8
□	10
◇	12

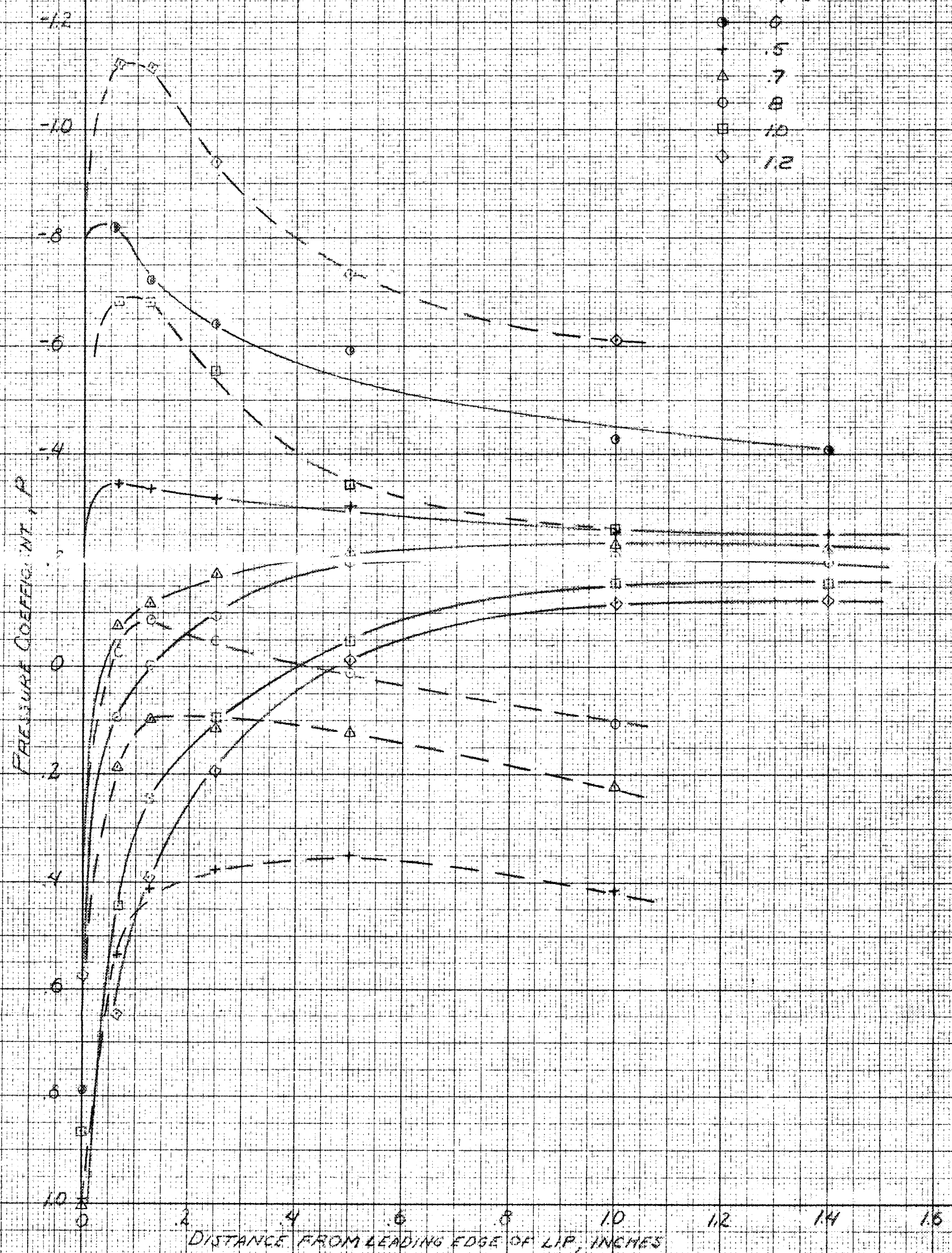


FIGURE 20.- PRESSURE-COEFFICIENT DISTRIBUTION FOR VARIOUS INLET-VELOCITY RATIOS WITH LIP 6 AT ZERO INCIDENCE FOR A 10° RAMP ANGLE.

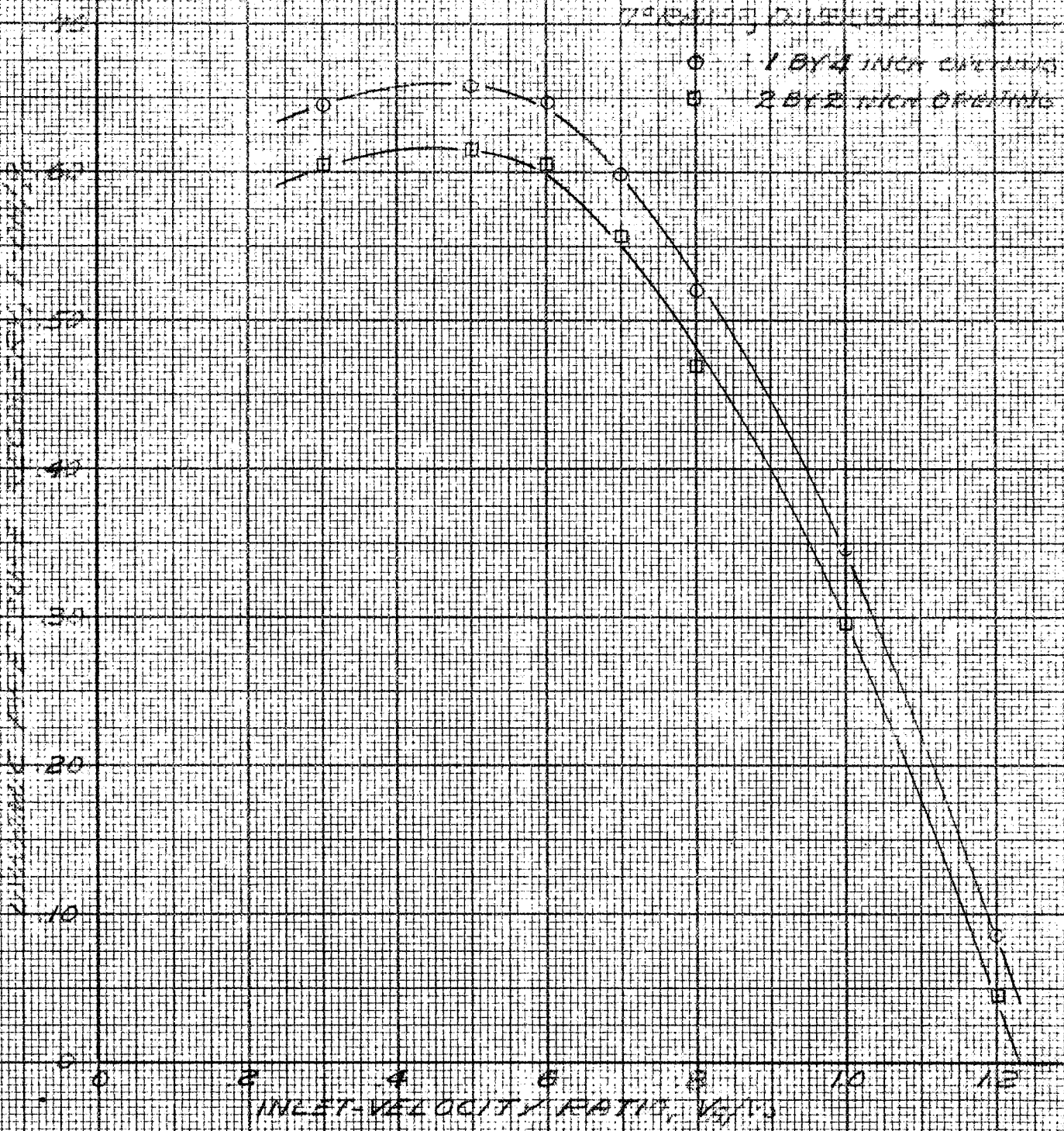


FIGURE 21 - THE RELATIONSHIP BETWEEN THE INLET-VELOCITY RATIO AND THE DIFFUSION EFFICIENCY FOR TWO DIFFERENT AIRFOIL SHAPES

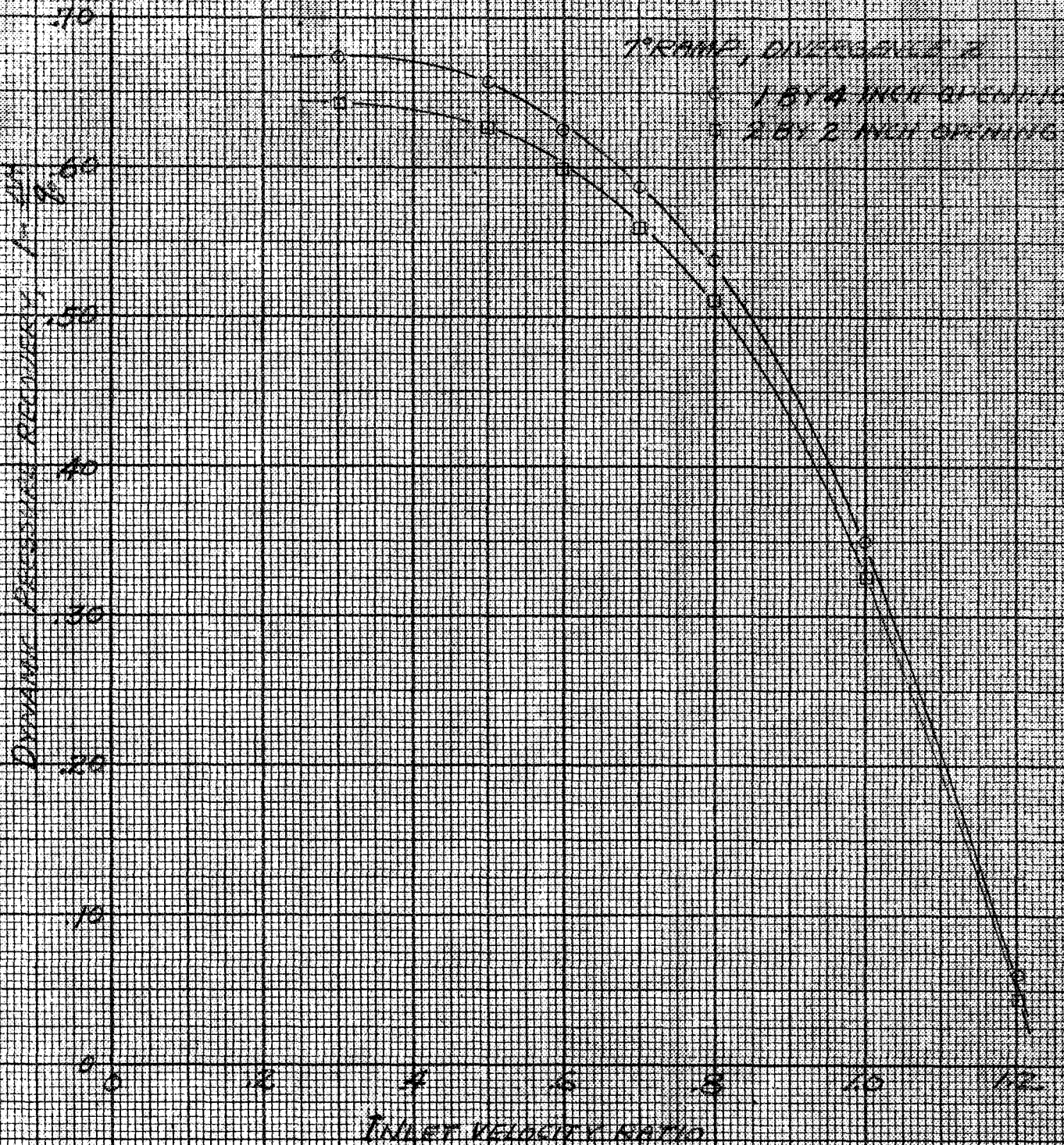


FIGURE 22 VARIATION OF DYNAMIC PRESSURE RECOVERY AFTER DIVERGENCE WITH INLET VELOCITY RATIO FOR TWO SUBMERGED INLET ENTRANCE SHAPES FOR DIVERGENCE ANGLE α .

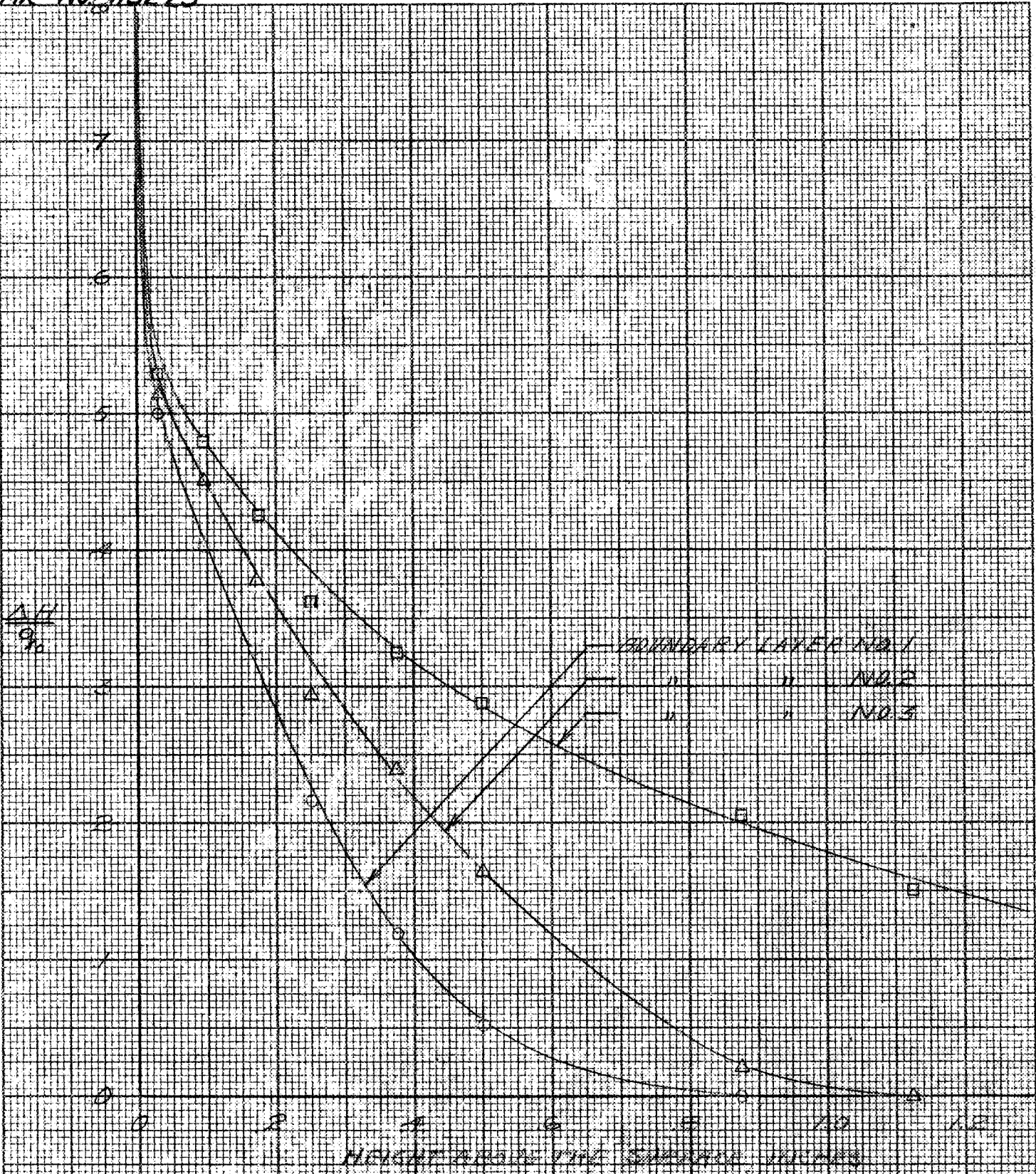


FIGURE 23. BOUNDARY LAYERS AND DUST SURVEILLANCE - DUST TESTS WIND TUNNEL

MR NO A5E23

ENGINE DESIGN CO NO 348 B

7° DIVERGING FAN NO 4
 O BOUNDARY LAYER NO 1
 A " " NO 2
 S " " NO 3

BOUNDARY LAYER THICKNESS

INLET VELOCITY FT/SEC, 1000

RA 127
53 770

LA-127 5-27-73

ASU IN OTHER

Figure 2A: The variation of boundary layer thickness
 after diffusion with inlet velocity ratio
 for three boundary layer thicknesses

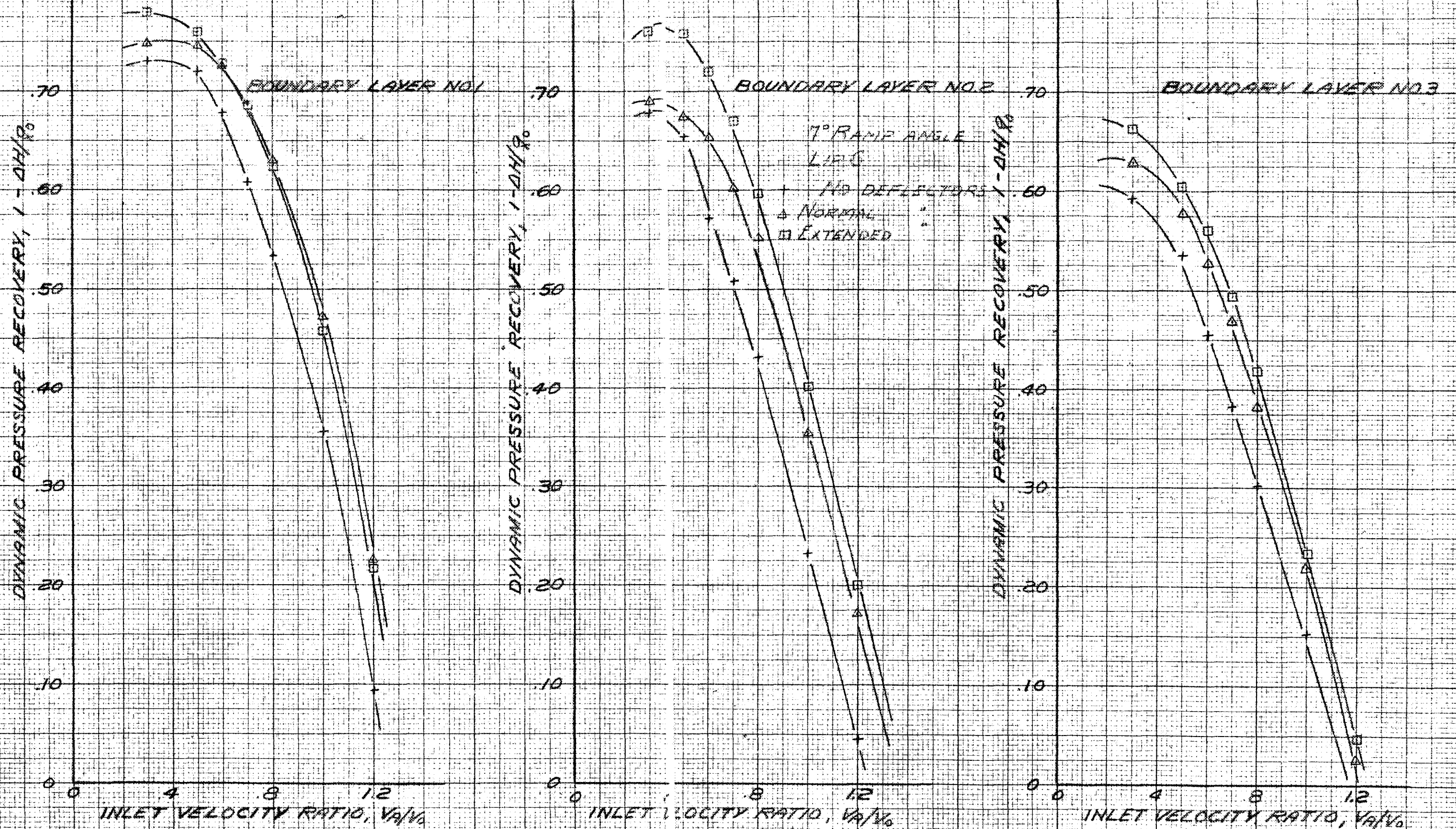


FIGURE 25. THE VARIATION OF DYNAMIC-PRESSURE RECOVERY AFTER DIFFUSION WITH INLET-VELOCITY RATIO FOR VARIOUS BOUNDARY LAYERS AND DEFLECTORS.

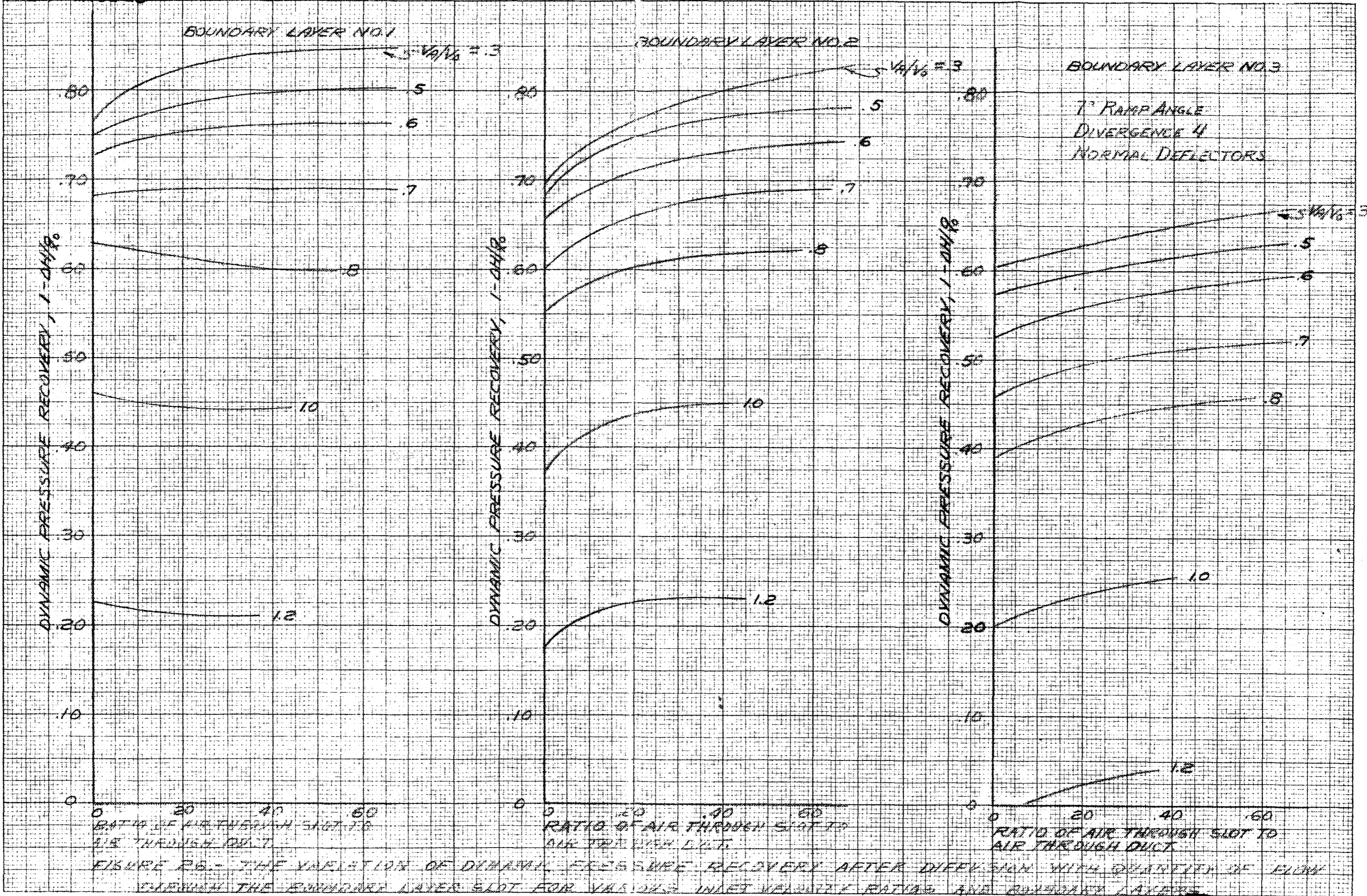
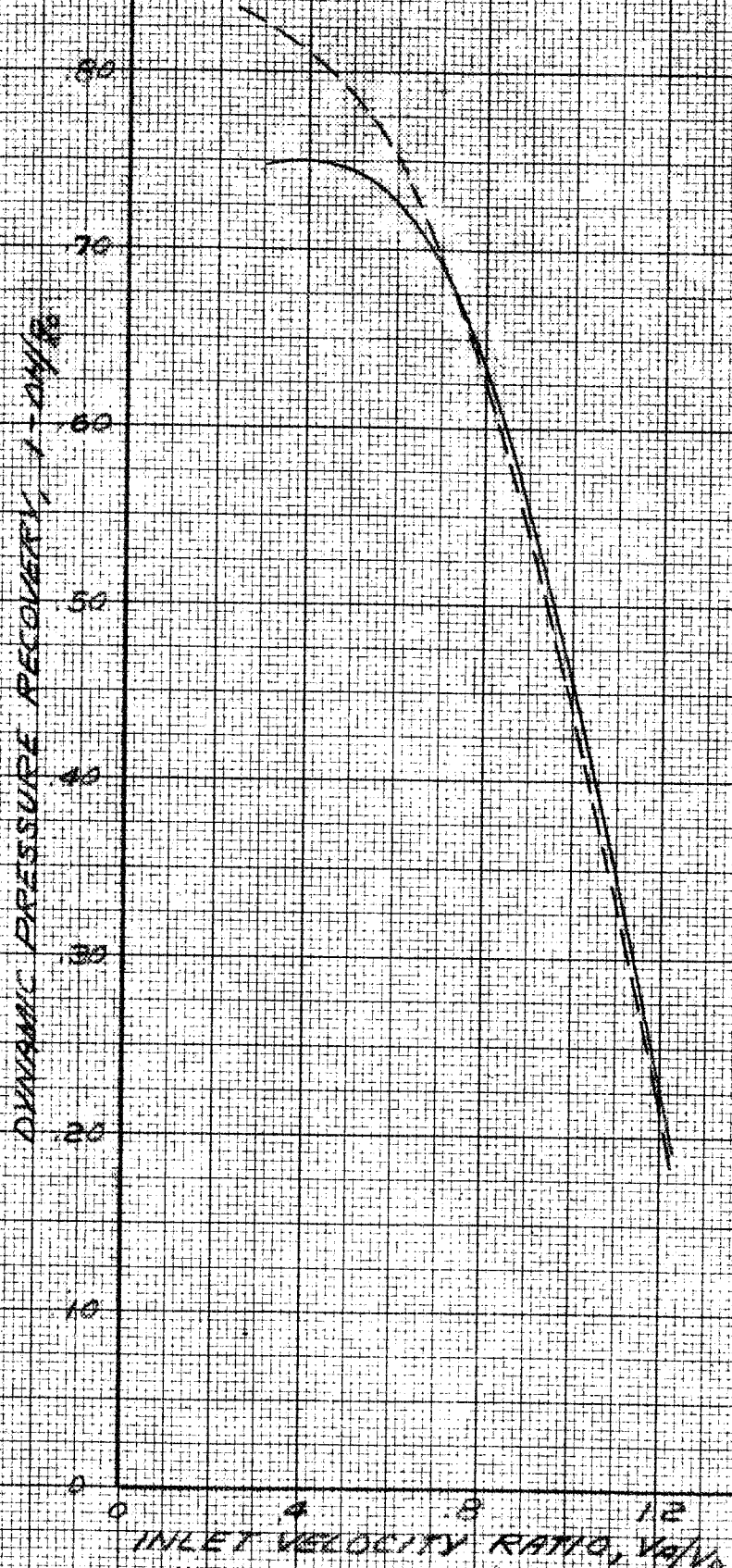
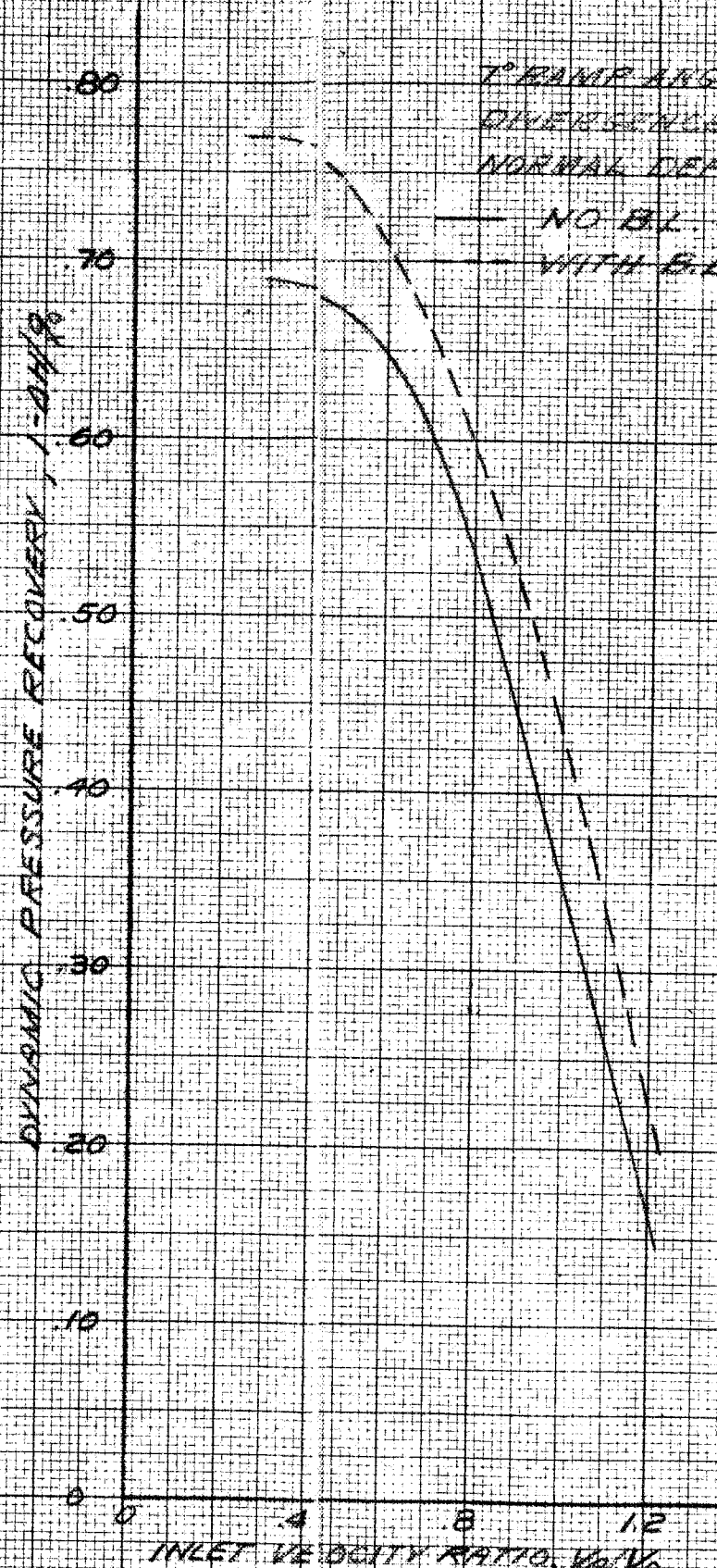


FIGURE 26 - THE VARIATION OF DYNAMIC PRESSURE RECOVERY AFTER DIFFUSION WITH QUANTITY OF FLOW THROUGH THE BOUNDARY LAYER SLOT FOR VARIOUS INLET VELOCITY RATIOS AND BOUNDARY LAYERS

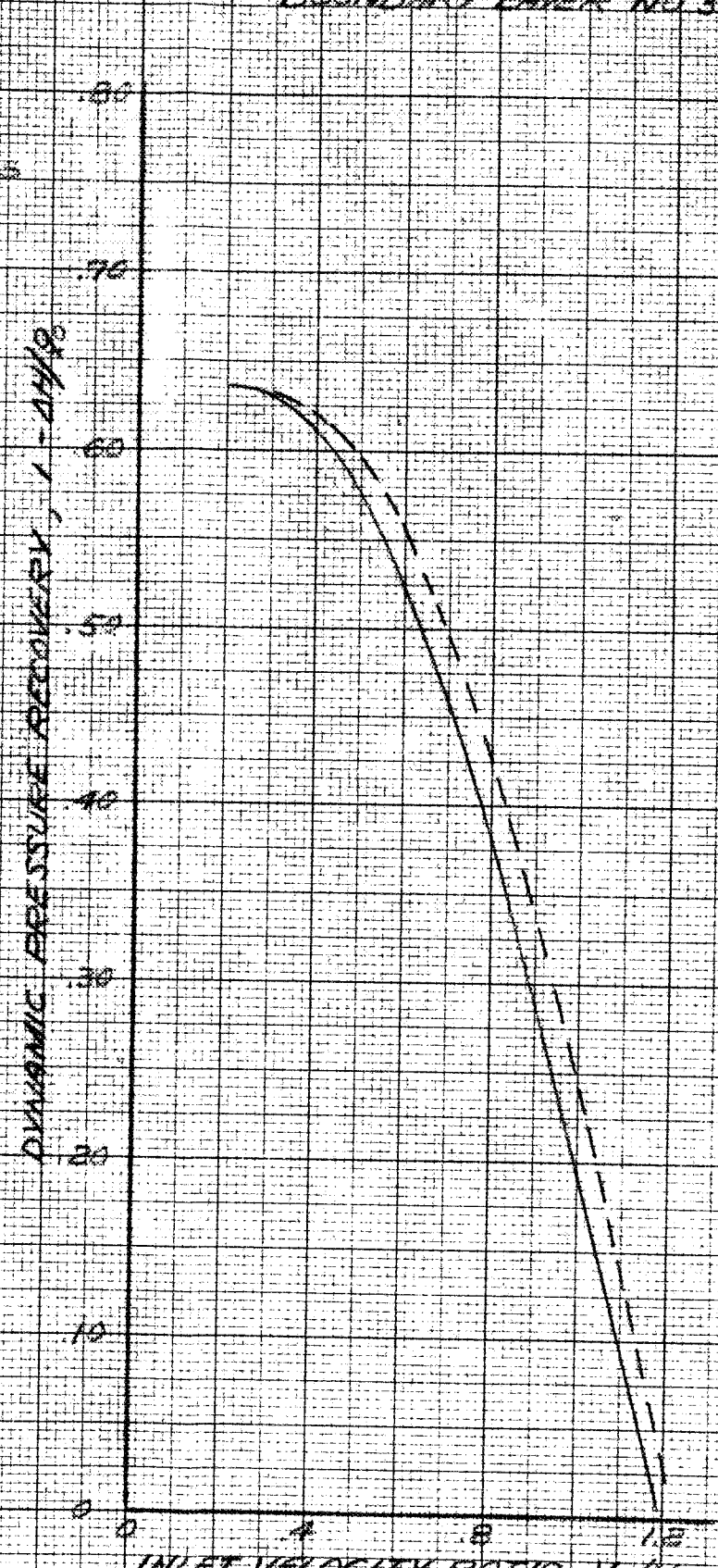
BOUNDARY LAYER NO. 1



BOUNDARY LAYER NO. 2



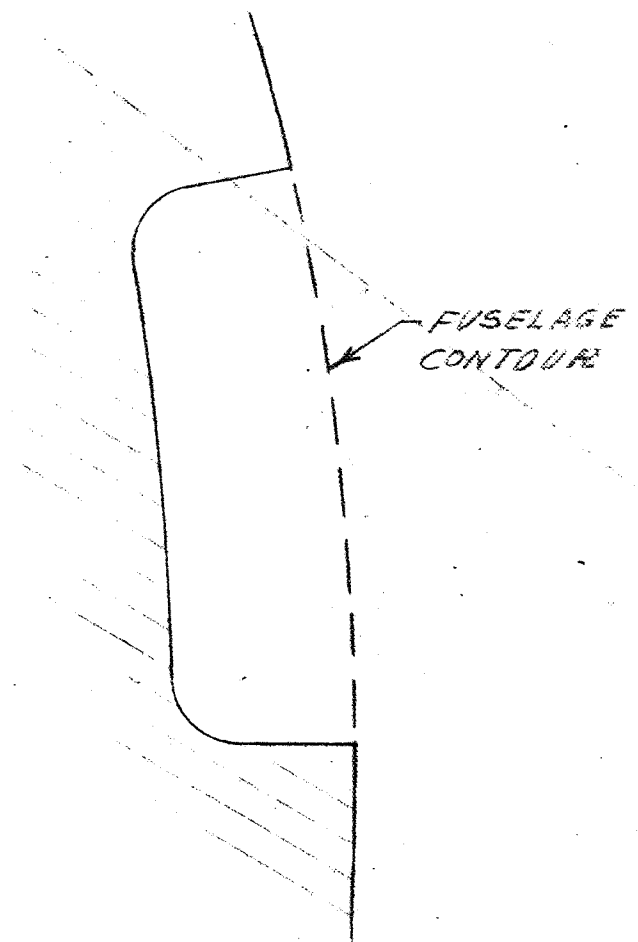
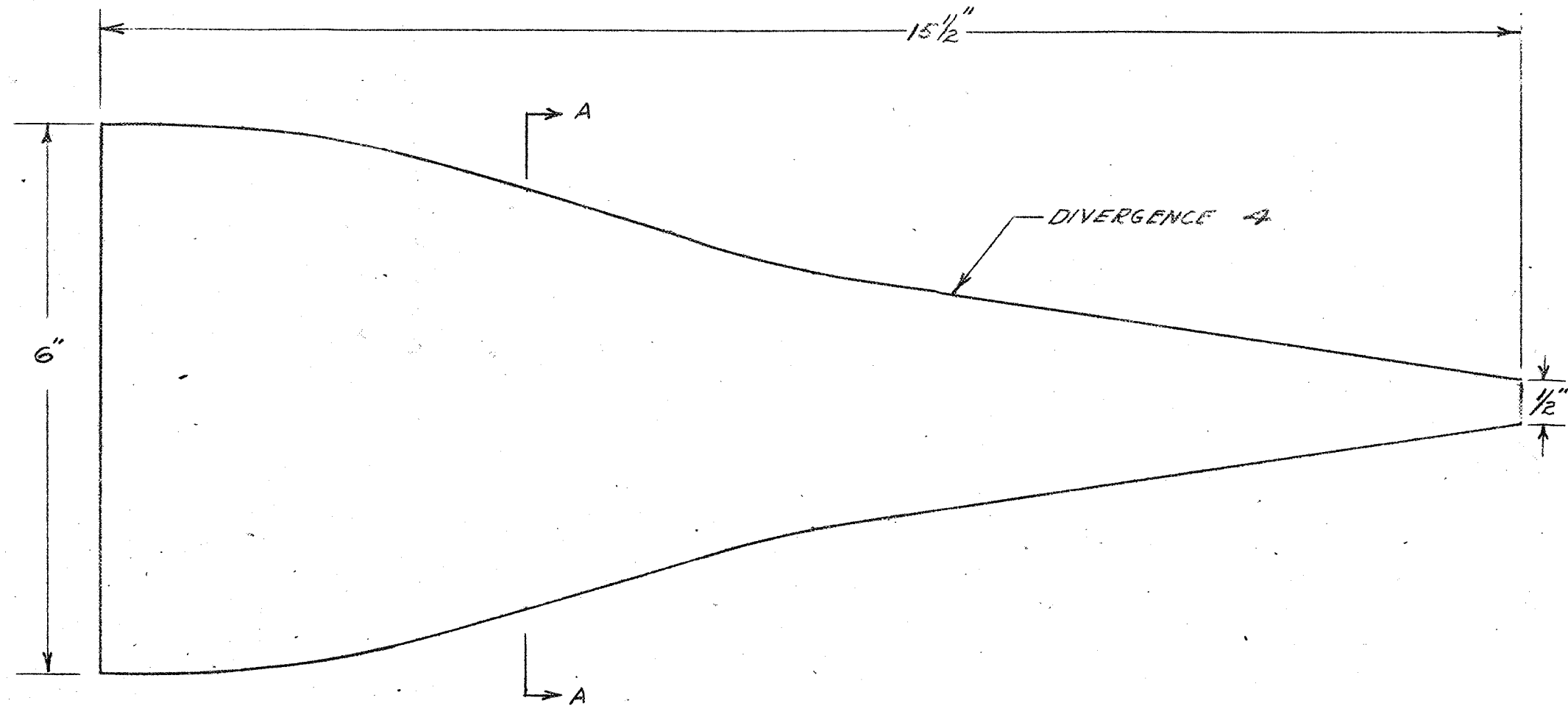
BOUNDARY LAYER NO. 3



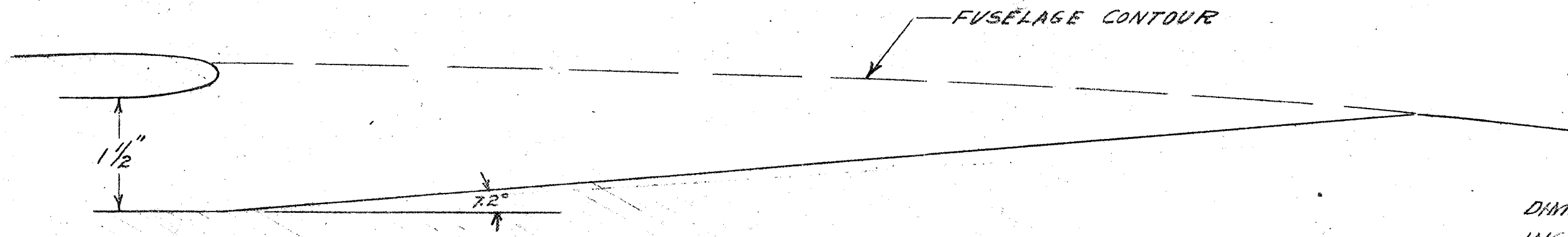
7° RAMP ANGLE
 DIVERGENCE 4°
 NORMAL DEFLECTORS
 — NO BL. SLOT
 - - - WITH BL. SLOT

FIGURE 27.— THE VARIATION OF DYNAMIC PRESSURE RECOVERY AFTER DIFFUSION WITH INLET VELOCITY RATIO FOR 80% OF THE INTAKE AIR DRAWN INTO THE BOUNDARY LAYER

100 179 (2017)



SECTION A-A
(TYPICAL)



DIMENSIONS ARE IN
INCHES MODEL SCALE.

FIGURE 28.- SKETCH OF THE SUBMERGED DUCT ENTRANCE INSTALLED ON THE .25-SCALE MODEL OF A FIGHTER AIRPLANE. NO DEFLECTORS.

MR NO 8523

DYNAMIC PRESSURE COEFFICIENT

120
90
60
30
0

NO DEFLECTORS
EXTENDED DEFLECTORS
NORMAL DEFLECTORS

NOTE: PRESSURE TUBES MOUNTED IN ENTRANCE FOR COMPARISON PURPOSES ONLY.

0 2 4 6 8 10 12
VELOCITY RATIO, V/V_0

FIGURE 29 - VARIATION OF DYNAMIC PRESSURE COEFFICIENT WITH INLET VELOCITY RATIO FOR VARIOUS DEFLECTOR CONFIGURATIONS SUBMERSED-JET INSTALLATION ON A 25-SCALE MODEL OF A FIGHTER AIRPLANE

MR NO. A5E23

ENGINE DESIGNER CO NO 348 B

NOTED
3/23/51

AM 11 30 (1)

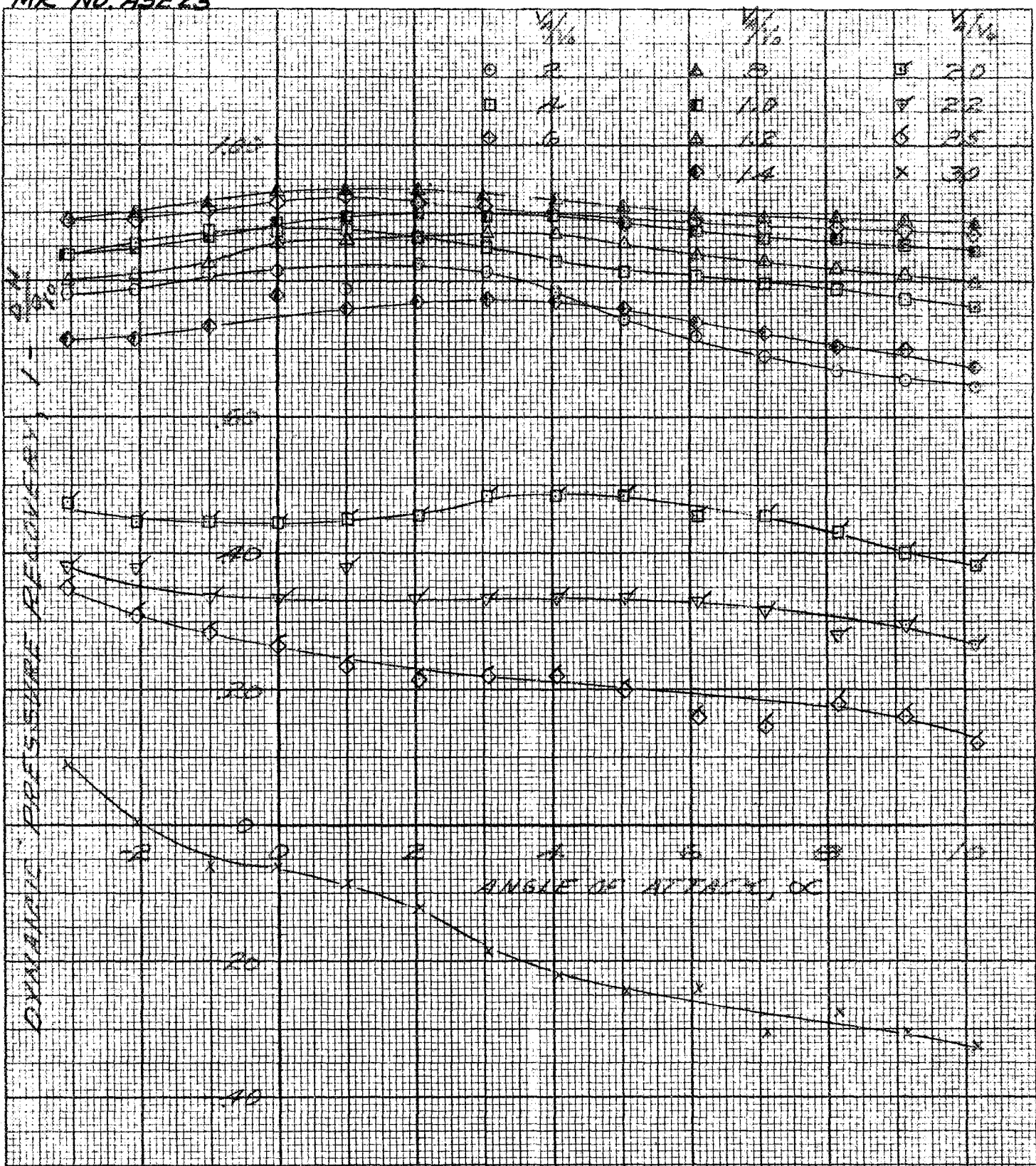


FIGURE 30.- DYNAMIC-PRESSURE RECOVERY OF THE 25-CELL MODEL OF A FIGHTER AIRPLANE WITH SUBMERSED DUCT ENTRANCES.

ACEL 11 01 01 01 01



MR. NO. 45E23

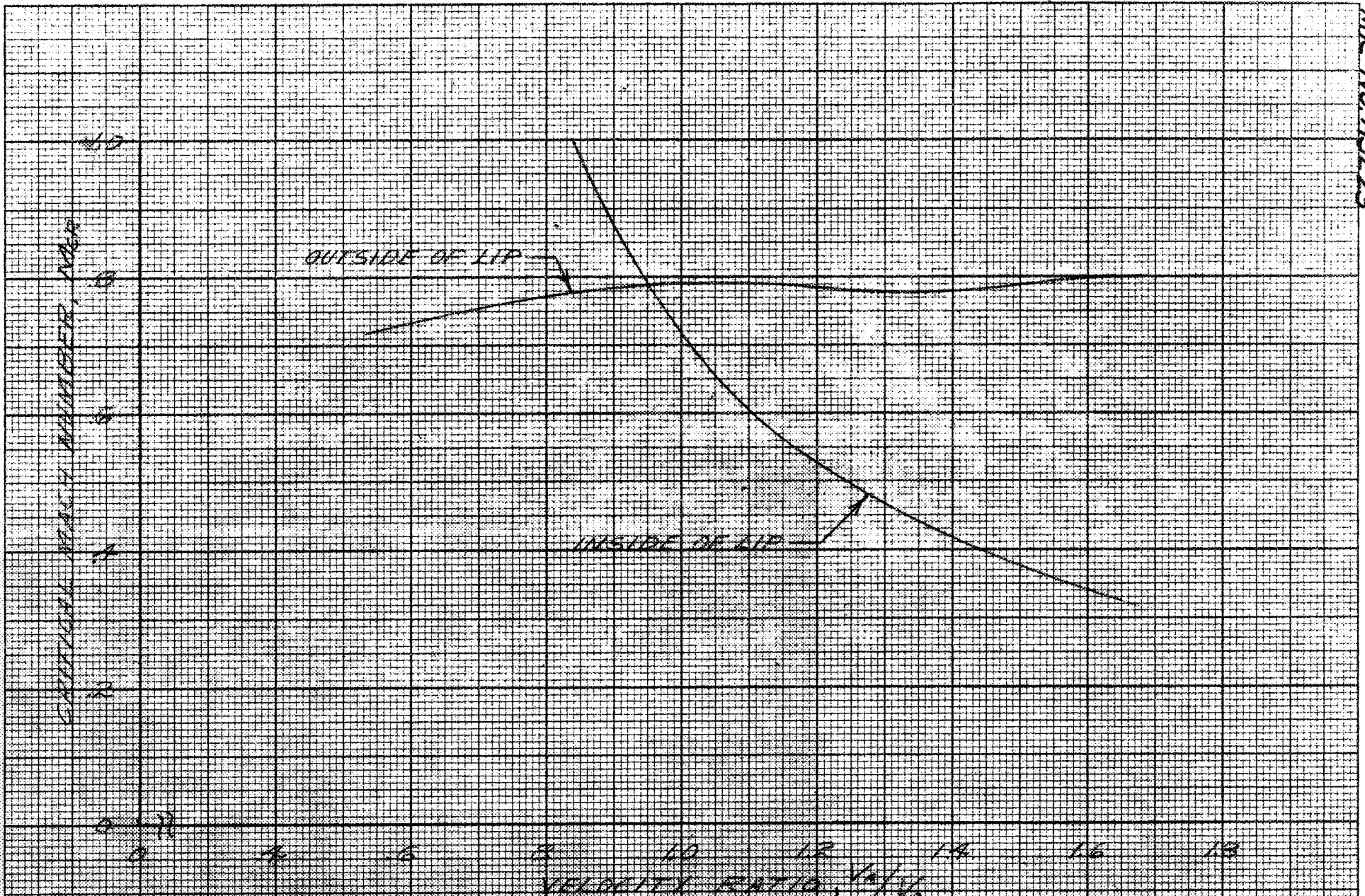


FIGURE 31 - VARIATION OF CRITICAL MACH NUMBER WITH INLET-VELOCITY RATIO FOR THE SUBMERGED-DUCT INSTALLATION ON THE 25% SCALE MODEL OF A FIGHTER AIRPLANE. MATCHED OPERATING CONDITIONS.

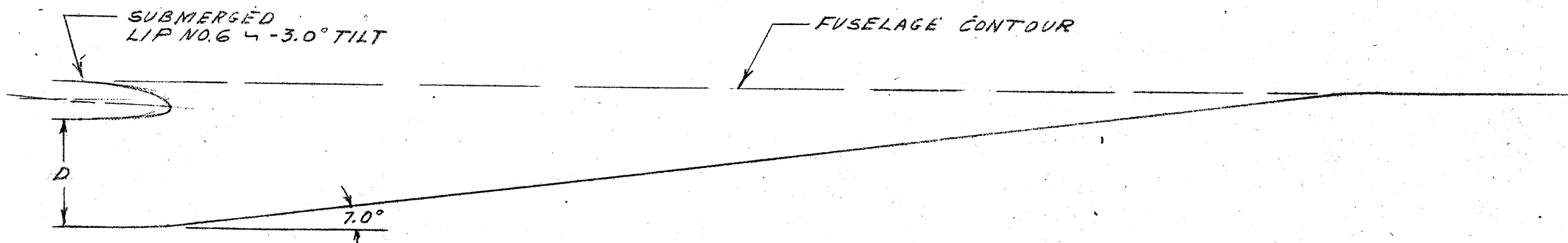
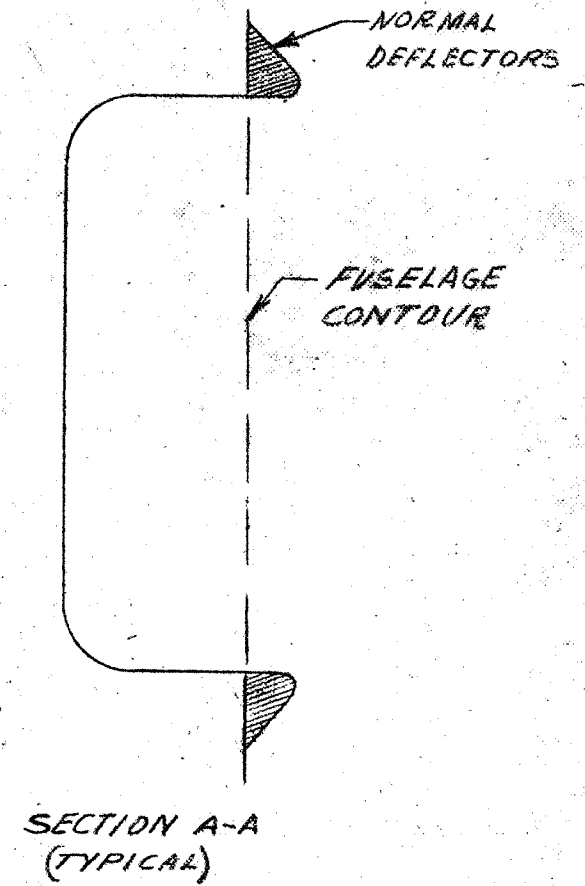
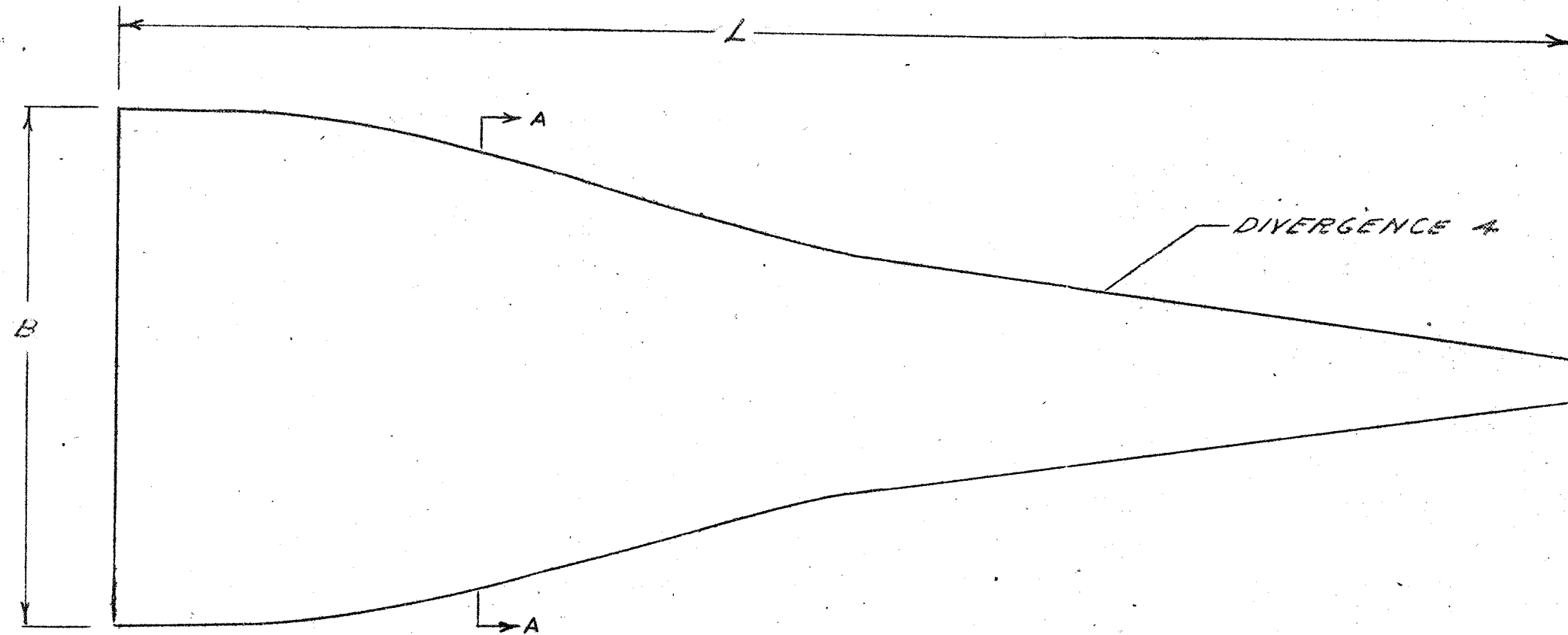


FIGURE 3R.— SKETCH OF SUBMERGED DUCT ENTRY FOR WHICH DESIGN DATA ARE GIVEN.

11-682 .OM .Y .M .NO .989-11
 KEUFFEL & ESSER CO., N. Y.
 10 X 10 to the inch, 516 lines accepted.
 Engraving 1 X 10 in.
 MADE IN U. S. A.

MR. NO. 85E23

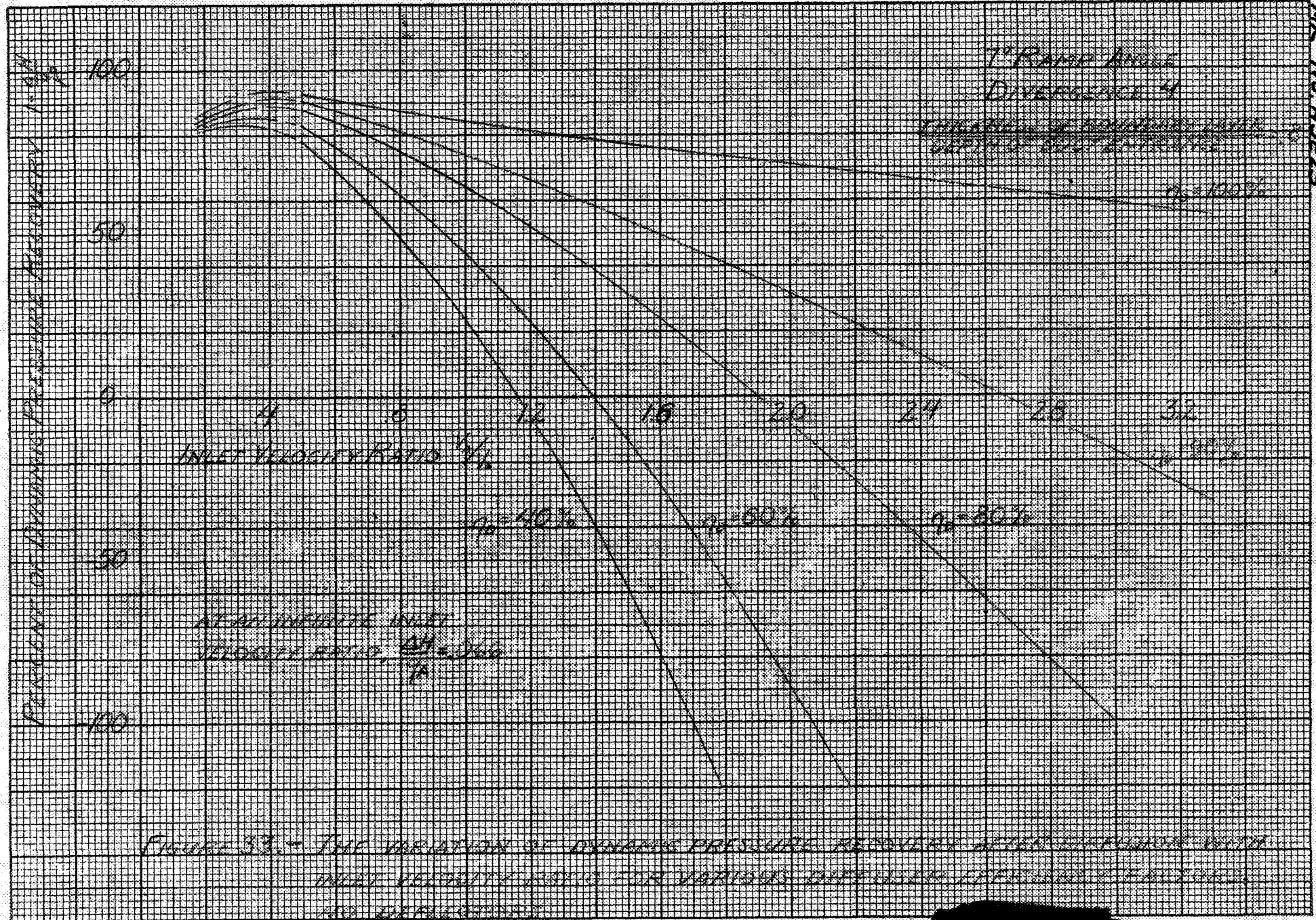


Figure 33.- The variation of dynamic pressure recovery after expansion with inlet velocity ratio for various diffuser efficiencies.

LA 171
23 513

MR NO. A5E23

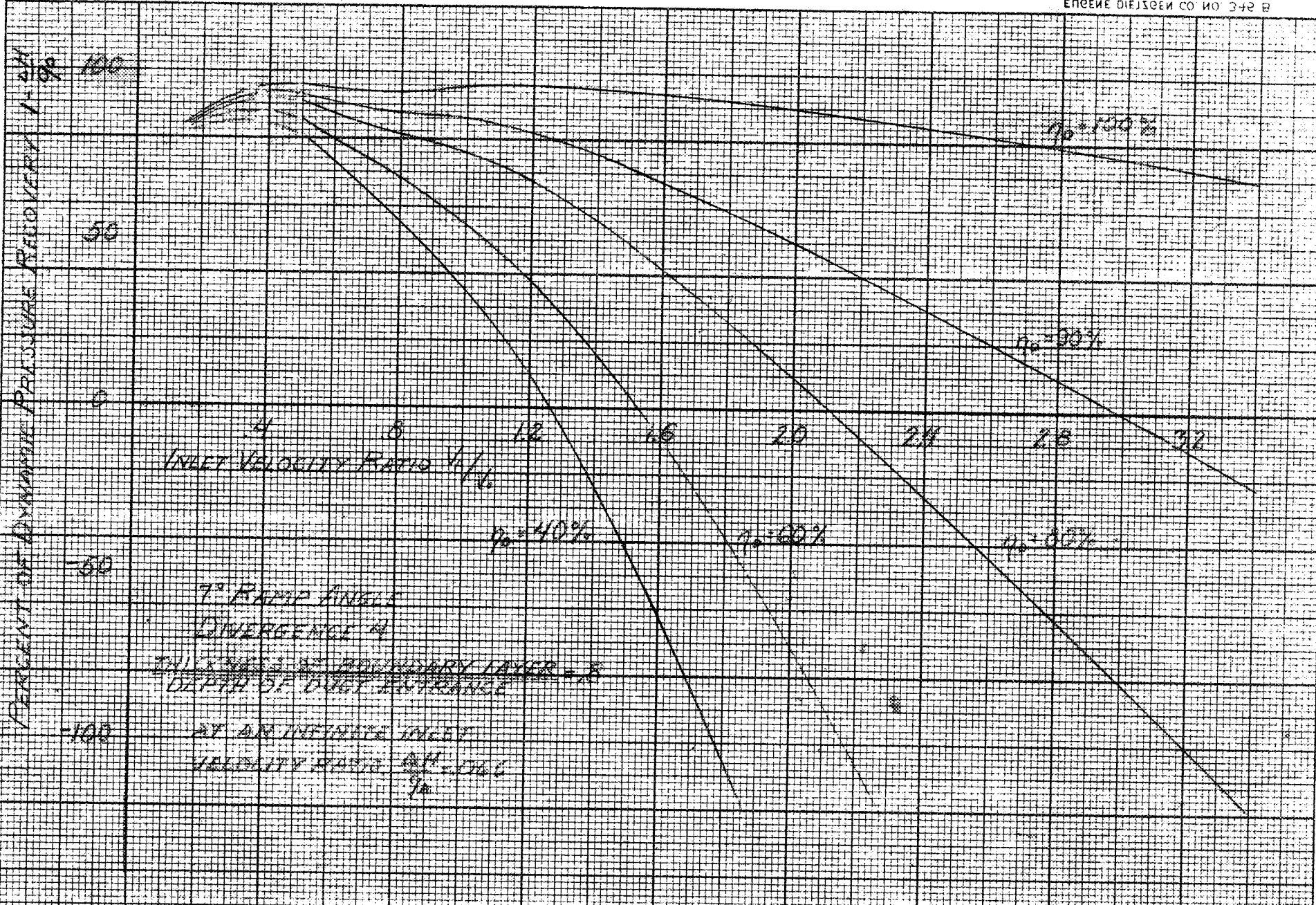
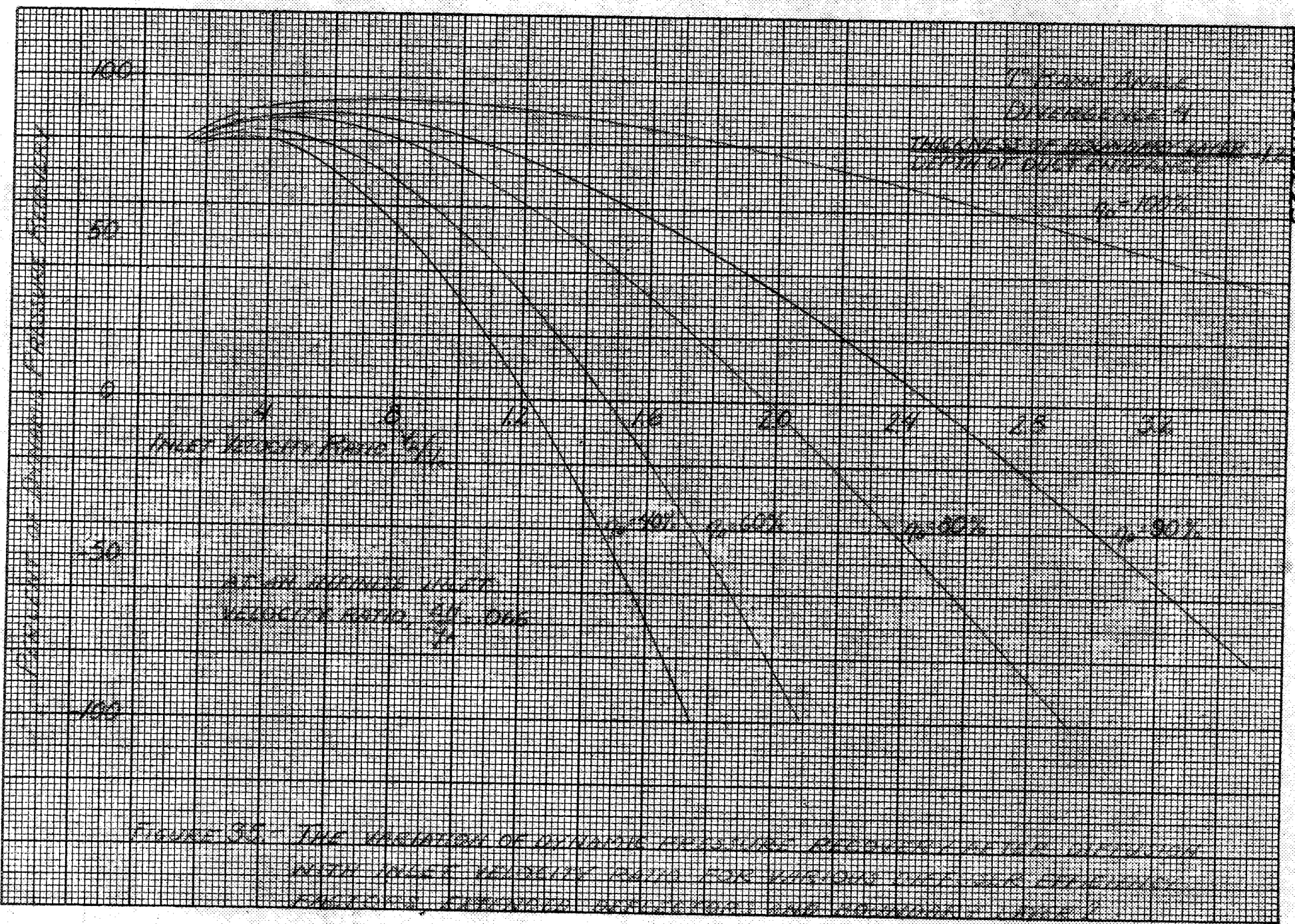


FIGURE 54- THE VARIATION OF DYNAMIC PRESSURE RECOVERY AFTER DIVERGENCE WITH INLET VELOCITY RATIO FOR VARIOUS DIFFUSER EFFICIENCY FACTORS, NORMAL DEFLECTION

REUPPEL & EBER CO., N. Y. NO. 388-11
 10 x 10 to the 4 inch. Grid lines centered.
 Engraving 1 x 10 in.
 MADE IN U. S. A.

MR. NO. A5523



157161
 53773
 KEFFER & ESSER CO., N. Y. N. O. NO. 389-11
 10 X 10 to the 1/2 inch grid lines extended.
 Engraving 7 X 10 in.
 MADE IN U. S. A.

MR. NO. R5E23

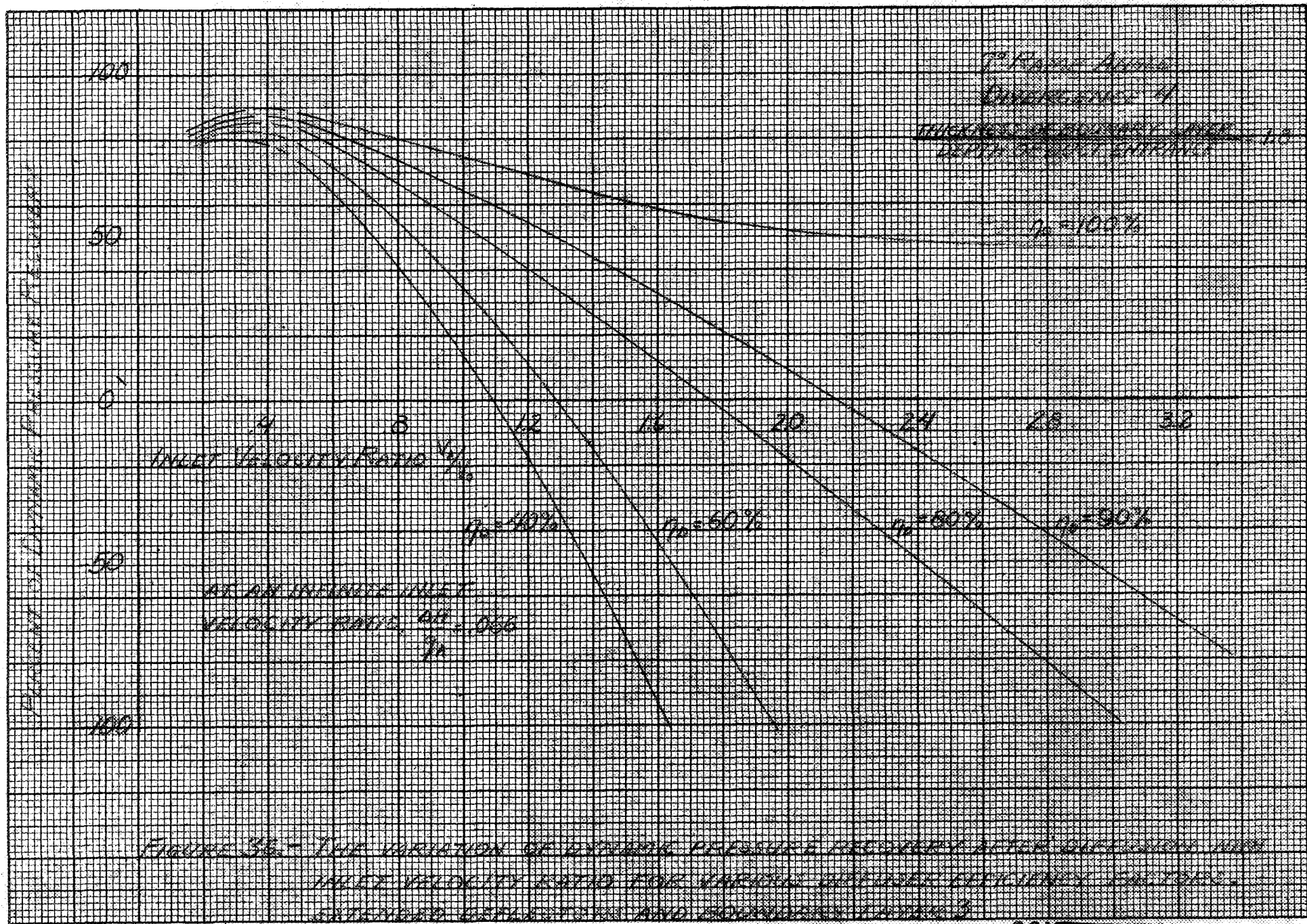


FIGURE 36. THE VARIATION OF PRESSURE RECOVERY AFTER SUPersonic FLOW INLET VELOCITY RATIO FOR VARIOUS INLET MACH NUMBERS.

MR No. A5E23

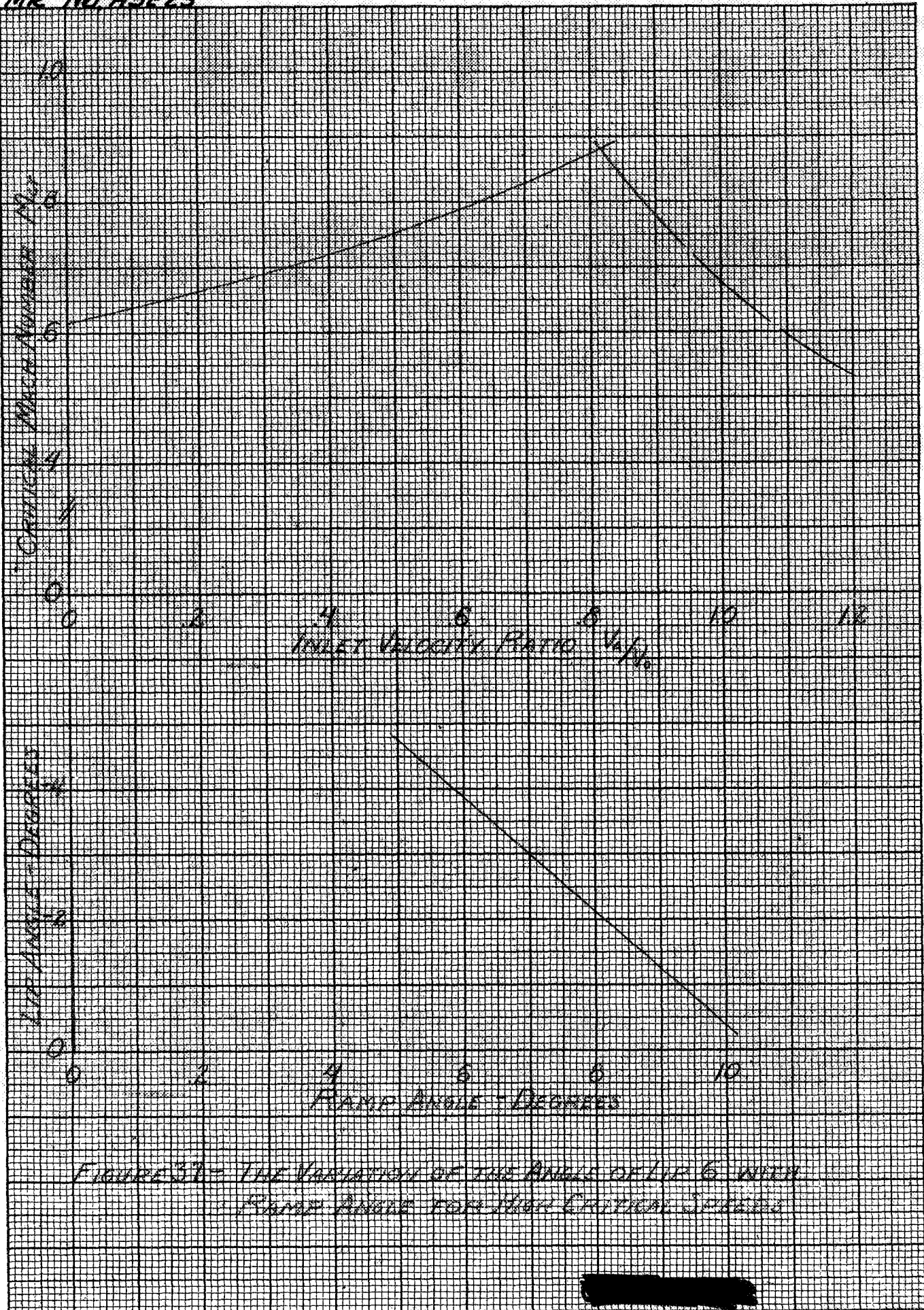


FIGURE 31 - THE VARIATION OF THE ANGLE OF LIFT α WITH RAMP ANGLE FOR HIGH CRITICAL SPEEDS

MADE IN U.S.A.
Guthrie, Inc. 1 x 10 in.
Ketchikan, Alaska
Ketchikan & Reed Co., N. Y. No. 38-11

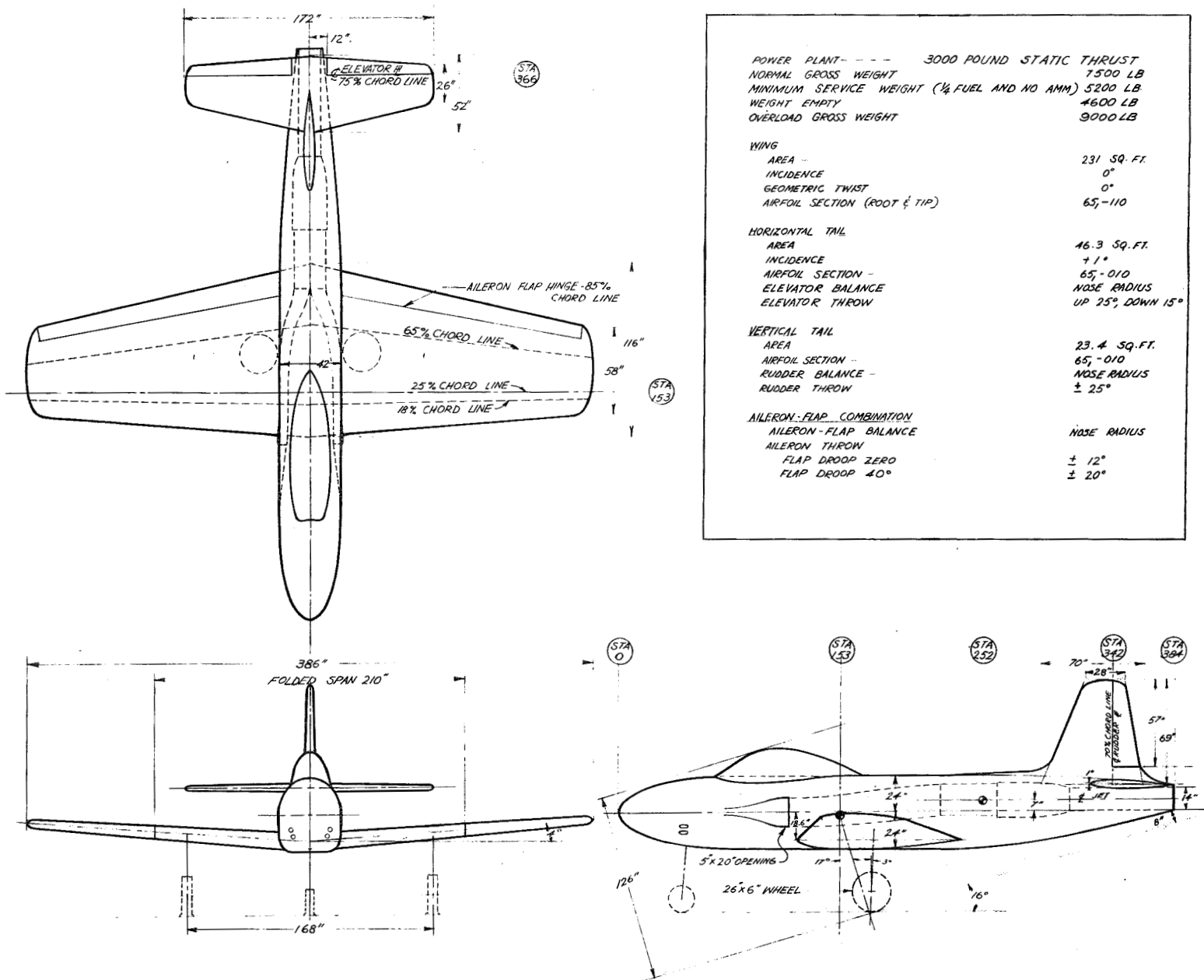


FIGURE 36. THREE-VIEW OF A HIGH-SPEED JET FIGHTER DESIGN.

MR NO A5E23

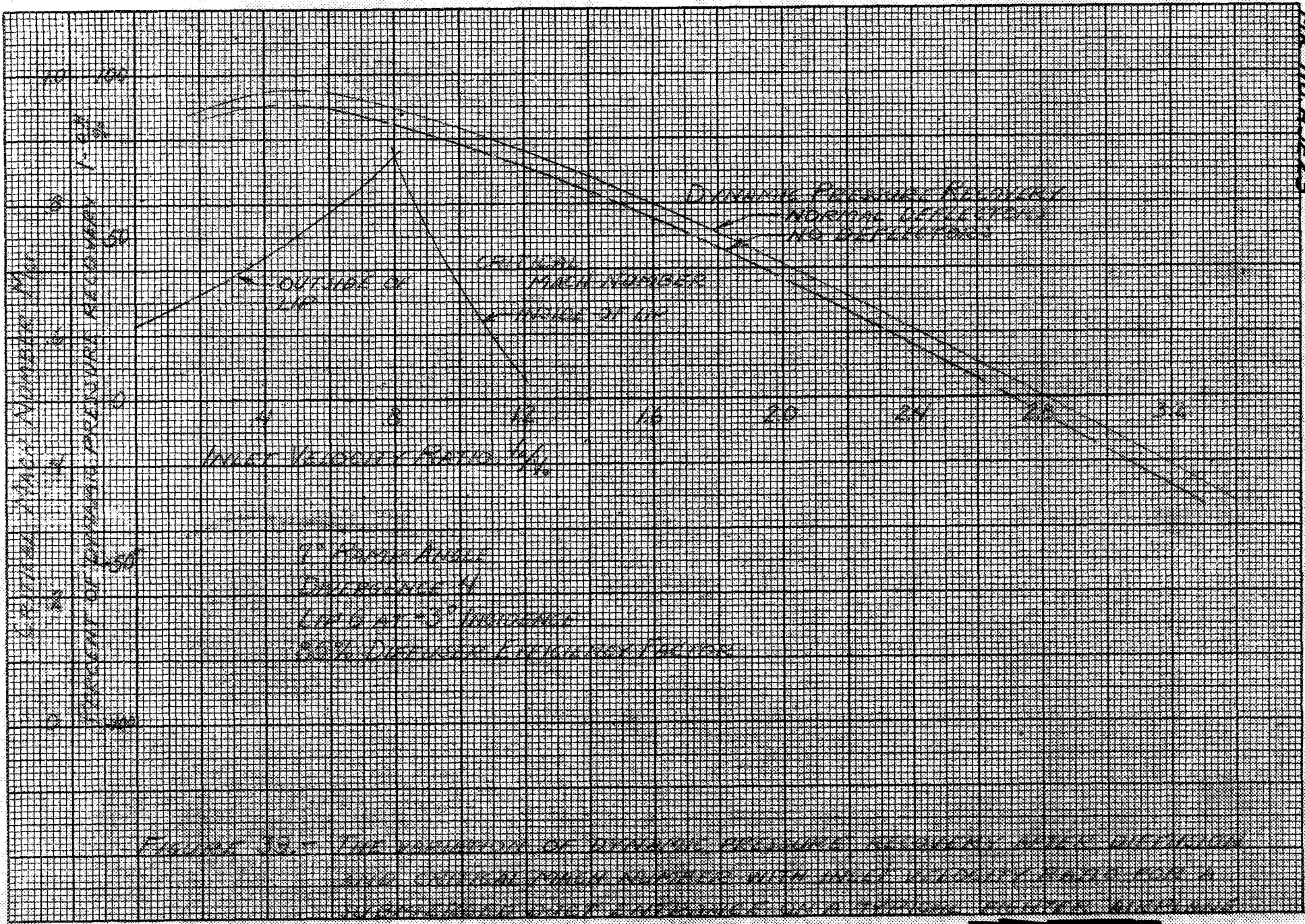


Figure 10. The variation of dynamic pressure recovery with Mach number for a 7.5 inch diameter tube with both ends open to atmosphere. The test was conducted at a pressure of 14.7 psia and a temperature of 59°F.